

Rare semileptonic $B \rightarrow K(\pi)l_i^-l_j^+$ decay in a vector leptoquark model

Murugeswaran Duraisamy

Department of Physics, Virginia Commonwealth University, Richmond, Virginia 23284, USA

Suchismita Sahoo and Rukmani Mohanta

School of Physics, University of Hyderabad, Hyderabad 500046, India

(Received 6 October 2016; published 17 February 2017)

We investigate the consequence of vector leptoquarks on the rare semileptonic lepton flavor violating decays of the B meson which are more promising and effective channels to probe the new physics signal. We constrain the resulting new leptoquark parameter space by using the branching ratios of $B_{s,d} \rightarrow l^+l^-$, $K_L \rightarrow l^+l^-$ and $\tau^- \rightarrow l^-\gamma$ processes. We estimate the branching ratios of rare lepton flavor violating $B \rightarrow K(\pi)l_i^-l_j^+$ processes using the constrained leptoquark couplings. We also compute the forward-backward asymmetries and the lepton nonuniversality parameters of the LFV decays in the vector leptoquark model. Furthermore, we study the effect of vector leptoquark on the $(g-2)_\mu$ anomaly.

DOI: [10.1103/PhysRevD.95.035022](https://doi.org/10.1103/PhysRevD.95.035022)**I. INTRODUCTION**

The discovery of the Higgs boson at LHC completes the standard model (SM) picture of particle interactions, which is quite successful in describing all the observed experimental data so far below the electroweak scale. Still, we need physics beyond it in order to solve the hierarchy and flavor problems. In this context, the study of rare B decay modes involving the flavor changing neutral current (FCNC) transitions, $b \rightarrow s/d$, are more captivating. The FCNC processes are highly suppressed in the SM and occur via one-loop level only. It should be noted that the current measured data by LHCb Collaboration on angular observables in rare B decays show significant deviation from the SM predictions. In particular, the discrepancy of 3σ in the famous P'_5 angular observable [1,2] and the decay rate [3] of rare $B \rightarrow K^*\mu^+\mu^-$ processes have become a tension in recent times. In addition, the ratio $R_K = \text{Br}(B \rightarrow K\mu^+\mu^-)/\text{Br}(B \rightarrow Ke^+e^-)$, canceling the hadronic uncertainties to a very large extent, has also a 2.6σ deviation from the SM prediction [4,5], thus indicates the violation of the lepton flavor universality (LFU). The decay rate of $B_s \rightarrow \phi\mu^+\mu^-$ process is also low (3σ deviation) compared to its SM value [6].

Within the SM of electroweak interactions, the generation lepton number is exactly conserved, since the neutrinos are deemed as massless particles. Nonetheless, the observation of neutrino oscillation has provided unambiguous evidence for lepton number violation in the neutral sector. The observation of lepton nonuniversality by the LHCb Collaboration generically implies the existence of lepton flavor violating (LFV) decay processes. Since the observed data on lepton nonuniversality is due to a 25% deficit in the muon channel, thus LFV is more for muonic processes than for electronic processes [7]. The branching ratio of $h \rightarrow \tau\mu$ LFV decay is found to be

$\text{Br}(h \rightarrow \tau\mu) = 0.84^{+0.39}_{-0.37}$ by the CMS Collaboration [8], which has a 2.6σ deviation from the SM value, thus boosted the interest of physicists to study more LFV decay processes in charged sector such as $l_i \rightarrow l_j\gamma$, $l_i \rightarrow l_jl_k\bar{l}_k$, $B_s \rightarrow l_i^\pm l_j^\mp$ and $B \rightarrow K^{(*)}l_i^\pm l_j^\mp$ etc. Theoretically, the LFV processes are free from the nonperturbative hadronic effects and significantly contribute some additional operators in comparison with the lepton flavor conserving (LFC) processes. In the literature, there are many attempts to analyze the LFV decays in the B sector in terms of various beyond the standard model scenarios [9–12]. Even though there is no direct experimental measurement on such LFV processes, but there exist upper bounds on some of these decays [13]. The observation of lepton flavor violating decays in upcoming and/or future experiments would provide evidence of new physics beyond the SM.

To settle the observed anomalies at LHCb using a specific theoretical framework, we extend the SM by adding a single vector leptoquark (LQ), which is a color triplet boson and arises naturally from the unification of quarks and leptons. LQs carry both baryon and lepton numbers and can be characterised by their fermion number, spin, and charge. Since the 1980s, LQs have been enthusiastically searched for without any positive results, although they could be produced directly at the colliders. The existence of an LQ can be found in many new physics (NP) models, such as the grand unified theories [14,15], Pati-Salam model, quark and lepton composite model [16], and the technicolor model [17]. The lepton and baryon number violating LQs are very heavy to avoid proton decay bounds. Nevertheless, the LQs having the baryon and lepton number conserving couplings do not allow proton decay and could be light enough to be seen in the current experiments. The interaction of an LQ with the SM fermions could be due to a scalar LQ doublet with

representation $(3, 2, 7/6)$ and $(3, 2, 1/6)$ or a vector LQ triplet $V_\mu^3(3, 3, 2/3)$, singlet $V_\mu^1(3, 1, 2/3)$ or doublet $V_\mu^2(\bar{3}, 2, 5/6)$ under the SM $SU(3)_C \times SU(2)_L \times U(1)_Y$ gauge group. In this work, we consider the vector LQ model which can produce both scalar and pseudoscalar operators in addition to the vector currents. We assume that the LQs conserve B and L quantum numbers and do not induce proton decay. We investigate the LFV $B \rightarrow K(\pi)l_i^- l_j^+$ processes in the context of vector LQ model. Even though the LFV processes occur at loop level with the presence of massless neutrinos in one of the loop or proceed via box diagrams, these can occur at tree level in the LQ model and are expected to have significantly large branching ratios. We compute the branching ratios and forward-backward asymmetries in these LFV processes. In addition, we also check the existence of lepton nonuniversality in the LQ model. The complete LQ phenomenology and the additional new physics contribution to the B sector has been investigated in the literature [10,11,18–24].

The paper is organized as follows. In Sec. II, we present the effective Hamiltonian describing the $b \rightarrow ql_i^- l_j^+$ transitions, where $q = s, d$. The angular distribution and the decay parameters of the semileptonic lepton flavor violating decays are described in Sec. III. In Sec. IV, we discuss the new physics contribution due to the exchange of vector LQ and the constraints on LQ couplings from $B_{s,d} \rightarrow l^+ l^-$, $K_L \rightarrow l^+ l^-$ and $\tau^- \rightarrow l^- \gamma$ processes are computed in Sec. V. The branching ratios, forward-backward asymmetries and the lepton nonuniversality of $B \rightarrow K(\pi)l_i^- l_j^+$ LFV decays are computed in Sec. VI. Finally, in Sec. VII, we explain the muon $g-2$ anomaly and the conclusions are summarized in Sec. VIII.

II. EFFECTIVE HAMILTONIAN FOR $b \rightarrow ql_i^- l_j^+$ PROCESSES

In this section, we discuss the effective Hamiltonian describing the FCNC $b \rightarrow q(=d, s)l_i^- l_j^+$ transitions. Here we will focus mainly on the $b \rightarrow sl_i^- l_j^+$ Hamiltonian as the $b \rightarrow dl_i^- l_j^+$ Hamiltonian can be obtained from it with the obvious replacements. The effective Hamiltonian for the quark-level transition $b \rightarrow sl_i^- l_j^+$ ($l = e, \mu, \tau$) in the SM is mainly given by [25]

$$\begin{aligned} \mathcal{H}_{\text{eff}}^{\text{SM}} = & -\frac{4G_F}{\sqrt{2}} V_{ts}^* V_{tb} \left[\sum_{i=1}^6 C_i(\mu) \mathcal{O}_i(\mu) \right. \\ & + C_7^{\text{SM}} \frac{e}{16\pi^2} [\bar{s}\sigma_{\mu\nu}(m_s P_L + m_b P_R)b] F^{\mu\nu} \\ & \left. + C_V^{\text{SM}} \frac{\alpha_{em}}{4\pi} (\bar{s}\gamma^\mu P_L b) L_{ij}^\mu + C_A^{\text{SM}} \frac{\alpha_{em}}{4\pi} (\bar{s}\gamma^\mu P_L b) L_{ij}^{5\mu} \right], \end{aligned} \quad (1)$$

where $L_{ij}^\mu = \bar{l}_i \gamma^\mu l_j$ and $L_{ij}^{5\mu} = \bar{l}_i \gamma^\mu \gamma_5 l_j$. Here G_F denotes the Fermi constant, $V_{qq'}$ are the Cabibbo-Kobayashi-Maskawa (CKM) matrix elements, α_{em} is the fine structure constant, and $P_{L,R} = (1 \mp \gamma_5)/2$ are the chirality projection operators. The operators \mathcal{O}_i ($i = 1, \dots, 6$) correspond to the tree-level current-current operators ($\mathcal{O}_{1,2}$), QCD penguin operators (\mathcal{O}_{3-6}) and C_i 's are the Wilson coefficients. For $i = j$, $C_{7,V,A}^{\text{SM}}$ represent the SM Wilson coefficients $C_{7,9,10}$ and for $i \neq j$ they will vanish.

The total effective Hamiltonian for processes involving the $b \rightarrow sl_i^- l_j^+$ transition, in the presence of new physics operators with all the possible Lorentz structures, can be expressed as

$$\mathcal{H}_{\text{eff}}(b \rightarrow sl_i^- l_j^+) = \mathcal{H}_{\text{eff}}^{\text{SM}} + \mathcal{H}_{\text{eff}}^{\text{VA}} + \mathcal{H}_{\text{eff}}^{\text{SP}} + \mathcal{H}_{\text{eff}}^{\text{T}}, \quad (2)$$

where $\mathcal{H}_{\text{eff}}^{\text{SM}}$ is the SM effective Hamiltonian as given in Eq. (1), and the NP contributions are given as

$$\begin{aligned} \mathcal{H}_{\text{eff}}^{\text{VA}} = & -N_F [C_V (\bar{s}\gamma^\mu P_L b) L_{ij}^\mu + C_A (\bar{s}\gamma^\mu P_L b) L_{ij}^{5\mu} \\ & + C'_V (\bar{s}\gamma^\mu P_R b) L_{ij}^\mu + C'_A (\bar{s}\gamma^\mu P_R b) L_{ij}^{5\mu}], \end{aligned} \quad (3)$$

$$\begin{aligned} \mathcal{H}_{\text{eff}}^{\text{SP}} = & -N_F [C_S (\bar{s} P_R b) L_{ij} + C_P (\bar{s} P_R b) L_{ij}^5 \\ & + C'_S (\bar{s} P_L b) L_{ij} + C'_P (\bar{s} P_L b) L_{ij}^5], \end{aligned} \quad (4)$$

$$\mathcal{H}_{\text{eff}}^{\text{T}} = -N_F [2C_T (\bar{s}\sigma_{\mu\nu} b) L_{ij}^{\mu\nu} + i2C_{T5} (\bar{s}\sigma_{\mu\nu} b) L_{ij}^{\mu\nu 5}], \quad (5)$$

where $N_F = \frac{G_F \alpha_{em}}{\sqrt{2}\pi} V_{tb} V_{ts}^*$, $L_{ij}^5 = \bar{l}_i \gamma_5 l_j$, and $L_{ij}^{\mu\nu 5} = 2i\bar{l}_i \sigma^{\mu\nu} \gamma_5 l_j$. Here we use $\sigma^{\mu\nu} \gamma_5 = -\frac{i}{2} \epsilon^{\mu\nu\alpha\beta} \sigma_{\alpha\beta}$ to calculate $L_{ij}^{\mu\nu 5}$. In the above expressions $C_i^{(l)}$, where $i = V, A, S, P$, and $C_{T(5)}$ are the NP effective couplings which are negligible in the SM and can only be generated using new physics beyond the SM.

III. THEORETICAL FRAMEWORK FOR $\bar{B} \rightarrow \bar{K}(\pi)l_i l_j$ DECAY PROCESSES

The semileptonic $\bar{B} \rightarrow \bar{K}l_i l_j$ decay involves the quark level $b \rightarrow sl_i^- l_j^+$ transitions as mediated by the effective Hamiltonian of the form in Eq. (2). The relevant kinematical variables describing this three-body decay are the invariant mass squared of the lepton pair $q^2 = (P_B - P_K)^2$, and the polar angle θ_l . Here P_B and P_K are the four-momenta of the B meson and K meson, respectively, and θ_l is the angle between the K and lepton l_i in the $l_i - l_j$ rest frame. The polar angle differential decay distribution in the momentum transfer squared q^2 for the process $\bar{B} \rightarrow \bar{K}l_i l_j$ can be written in the form

$$\frac{d^2\Gamma}{dq^2 d\cos\theta_l} = \frac{G_F^2 \alpha_{em}^2 \beta_{ij} \sqrt{\lambda} |V_{tb} V_{ts}^*|^2}{2^{12} \pi^5 M_B^3} \sum_{i=1}^{12} I_i(\cos\theta_l), \quad (6)$$

where $\beta_{ij} = \sqrt{(1 - \frac{(m_i+m_j)^2}{q^2})(1 - \frac{(m_i-m_j)^2}{q^2})}$ and the kinematical factor $\lambda = M_B^4 + M_K^4 + q^4 - 2(M_B^2 M_K^2 + M_K^2 q^2 + M_B^2 q^2)$. The twelve angular coefficients $I_i(\cos\theta_l)$ appearing in the angular distribution depend on the couplings, kinematic variables, form factors, and the polar angle θ_l , which are defined as

$$I_1 = 2 \left[\left(1 - \frac{(m_i - m_j)^2}{q^2} \right) (q^2 - (q^2 - (m_i + m_j)^2) \cos^2 \theta_l) |H_V^0|^2 + 4k \frac{(m_i^2 - m_j^2)}{\sqrt{q^2}} \text{Re}[H_V^0 H_V^{0r*}] \cos \theta_l + \frac{(m_i - m_j)^2}{q^2} (q^2 - (m_i + m_j)^2) |H_V^l|^2 \right], \quad (7)$$

$$I_2 = 2 \left[\left(1 - \frac{(m_i + m_j)^2}{q^2} \right) (q^2 - (q^2 - (m_i - m_j)^2) \cos^2 \theta_l) |H_A^0|^2 + 4k \frac{(m_i^2 - m_j^2)}{\sqrt{q^2}} \text{Re}[H_A^0 H_A^{0r*}] \cos \theta_l + \frac{(m_i + m_j)^2}{q^2} (q^2 - (m_i - m_j)^2) |H_A^l|^2 \right], \quad (8)$$

$$I_3 = 2(q^2 - (m_i + m_j)^2) |H_S|^2, \quad (9)$$

$$I_4 = 2(q^2 - (m_i - m_j)^2) |H_P|^2, \quad (10)$$

$$I_5 = 8 \left(1 - \frac{(m_i - m_j)^2}{q^2} \right) ((m_i + m_j)^2 + (q^2 - (m_i + m_j)^2) \cos^2 \theta_l) |H_T^{0r}|^2, \quad (11)$$

$$I_6 = 32 \left(1 - \frac{(m_i + m_j)^2}{q^2} \right) ((m_i - m_j)^2 + (q^2 - (m_i - m_j)^2) \cos^2 \theta_l) |H_{TE}^{0r}|^2, \quad (12)$$

$$I_7 = 4\text{Re} \left[2k(m_i + m_j) H_V^0 H_S^* \cos \theta_l + \frac{(m_i - m_j)}{\sqrt{q^2}} (q^2 - (m_i + m_j)^2) H_V^l H_S^* \right], \quad (13)$$

$$I_8 = 4\text{Re} \left[2k(m_i - m_j) H_A^0 H_P^* \cos \theta_l + \frac{(m_i + m_j)}{\sqrt{q^2}} (q^2 - (m_i - m_j)^2) H_A^l H_P^* \right], \quad (14)$$

$$I_9 = -8\text{Re} \left[2k(m_i - m_j) H_V^l H_T^{0r*} \cos \theta_l + \frac{(m_i + m_j)}{\sqrt{q^2}} (q^2 - (m_i - m_j)^2) H_V^0 H_T^{0r*} \right], \quad (15)$$

$$I_{10} = 16\text{Re} \left[2k(m_i + m_j) H_A^l H_{TE}^{0r*} \cos \theta_l + \frac{(m_i - m_j)}{\sqrt{q^2}} (q^2 - (m_i + m_j)^2) H_0^l H_{TE}^{0r*} \right], \quad (16)$$

$$I_{11} = -16k \sqrt{q^2} \text{Re}[H_S H_T^{0r*}] \cos \theta_l, \quad (17)$$

$$I_{12} = 32k \sqrt{q^2} \text{Re}[H_P H_{TE}^{0r*}] \cos \theta_l. \quad (18)$$

Here $k = (\beta_{ij} \sqrt{q^2})/2$ is the lepton momentum and the expressions for the helicity amplitudes are given as

$$H_V^0 = \sqrt{\frac{\lambda}{q^2}} \left[(C_V^{\text{SM}} + C_V + C_V') f_+(q^2) + 2C_7^{\text{SM}} m_b \frac{f_T}{M_B + M_K} \right], \quad (19)$$

$$H_V^l = \frac{M_B^2 - M_K^2}{\sqrt{q^2}} (C_V^{\text{SM}} + C_V + C_V') f_0(q^2), \quad (20)$$

$$H_A^0 = \sqrt{\frac{\lambda}{q^2}} (C_A^{\text{SM}} + C_A + C_A') f_+(q^2), \quad (21)$$

$$H_A^l = \frac{M_B^2 - M_K^2}{\sqrt{q^2}} (C_A^{\text{SM}} + C_A + C_A') f_0(q^2), \quad (22)$$

$$H_S = \frac{M_B^2 - M_K^2}{m_b} (C_S + C_S') f_0(q^2), \quad (23)$$

$$H_P = \frac{M_B^2 - M_K^2}{m_b} (C_P + C_P') f_0(q^2), \quad (24)$$

$$H_T^{0r} = -2C_T \frac{\sqrt{\lambda}}{M_B + M_K} f_T(q^2), \quad (25)$$

$$H_{T5}^{0r} = -2C_{T5} \frac{\sqrt{\lambda}}{M_B + M_K} f_T(q^2). \quad (26)$$

The above expressions are calculated by using the parametrizations of matrix elements of the various hadronic currents between the initial B meson and the final K meson, in terms of the form factors f_0 , f_+ , and f_T as [5]

$$\langle \bar{K}(P_K) | \bar{s} \gamma^\mu b | \bar{B}(P_B) \rangle = f_+(q^2) (P_B + P_K)^\mu + [f_0(q^2) - f_+(q^2)] \frac{M_B^2 - M_K^2}{q^2} q^\mu, \quad (27)$$

$$\begin{aligned} & \langle \bar{K}(P_K) | \bar{s} \sigma^{\mu\nu} b | \bar{B}(P_B) \rangle \\ &= i \frac{f_T(q^2)}{M_B + M_K} [(P_B + P_K)^\mu q^\nu - q^\mu (P_B + P_K)^\nu]. \end{aligned} \quad (28)$$

It should be noted that, in general, the angular coefficients of semileptonic decays take the form

$$I_i(\cos \theta_l) = a_i + b_i \cos \theta_l + c_i \cos^2 \theta_l. \quad (29)$$

The differential decay rate for the decay $\bar{B} \rightarrow \bar{K} l_i l_j$ can be found by integrating over the polar angle in Eq. (6) to get

$$\frac{d\Gamma}{dq^2} = \frac{G_F^2 \alpha_{em}^2 \beta_{ij} \sqrt{\lambda} |V_{tb} V_{ts}^*|^2}{2^{12} \pi^5 M_B^3} \sum_{i=1}^{10} J_i, \quad (30)$$

where the coefficients $J_i = \int_{-1}^1 I_i(\cos \theta_l) d \cos \theta_l$ are given below as

$$\begin{aligned} J_1 = 4 & \left[\left(1 - \frac{(m_i - m_j)^2}{q^2} \right) \frac{1}{3} (2q^2 + (m_i + m_j)^2) |H_V^0|^2 \right. \\ & \left. + \frac{(m_i - m_j)^2}{q^2} (q^2 - (m_i + m_j)^2) |H_V^t|^2 \right], \end{aligned} \quad (31)$$

$$\begin{aligned} J_2 = 4 & \left[\left(1 - \frac{(m_i + m_j)^2}{q^2} \right) \frac{1}{3} (2q^2 + (m_i - m_j)^2) |H_A^0|^2 \right. \\ & \left. + \frac{(m_i + m_j)^2}{q^2} (q^2 - (m_i - m_j)^2) |H_A^t|^2 \right], \end{aligned} \quad (32)$$

$$J_3 = 4(q^2 - (m_i + m_j)^2) |H_S|^2, \quad (33)$$

$$J_4 = 4(q^2 - (m_i - m_j)^2) |H_P|^2, \quad (34)$$

$$J_5 = 16 \left(1 - \frac{(m_i - m_j)^2}{q^2} \right) \frac{1}{3} (2(m_i + m_j)^2 + q^2) |H_T^{0r}|^2, \quad (35)$$

$$J_6 = 64 \left(1 - \frac{(m_i + m_j)^2}{q^2} \right) \frac{1}{3} (2(m_i - m_j)^2 + q^2) |H_{TE}^{0r}|^2, \quad (36)$$

$$J_7 = 8 \frac{(m_i - m_j)}{\sqrt{q^2}} (q^2 - (m_i + m_j)^2) \text{Re}[H_V^t H_S^*], \quad (37)$$

$$J_8 = 8 \frac{(m_i + m_j)}{\sqrt{q^2}} (q^2 - (m_i - m_j)^2) \text{Re}[H_A^t H_P^*], \quad (38)$$

$$J_9 = -16 \frac{(m_i + m_j)}{\sqrt{q^2}} (q^2 - (m_i - m_j)^2) \text{Re}[H_V^0 H_T^{0r*}], \quad (39)$$

$$J_{10} = 32 \frac{(m_i - m_j)}{\sqrt{q^2}} (q^2 - (m_i + m_j)^2) \text{Re}[H_0^t H_{TE}^{0r*}]. \quad (40)$$

Here the coefficients $J_{11} = J_{12} = 0$. Next, we define the forward-backward asymmetry (A_{FB}) for the leptons by integrating over $\cos \theta_l$ in Eq. (6) as

$$\begin{aligned} A_{FB}(q^2) = & \left(\int_0^1 d \cos \theta_l \frac{d^2 \Gamma}{dq^2 d \cos \theta_l} \right. \\ & \left. - \int_{-1}^0 d \cos \theta_l \frac{d^2 \Gamma}{dq^2 d \cos \theta_l} \right) / \frac{d\Gamma}{dq^2}. \end{aligned} \quad (41)$$

After integration, we obtain

$$A_{FB}(q^2) = \frac{X}{\sum_{i=1}^{10} J_i}, \quad (42)$$

where the quantity X is defined as

$$\begin{aligned} X = 8k \text{Re} & \left[\frac{(m_i^2 - m_j^2)}{\sqrt{q^2}} (H_V^0 H_V^{t*} + H_A^0 H_A^{t*}) \right. \\ & + (m_i + m_j) (H_V^0 H_S^* + 4H_A^t H_{TE}^{0r*}) \\ & + (m_i - m_j) (H_A^0 H_P^* - 2H_V^t H_T^{0r*}) \\ & \left. - 2\sqrt{q^2} (H_S^0 H_T^{0r*} - 2H_P H_{TE}^{0r*}) \right]. \end{aligned} \quad (43)$$

Another interesting observable is the lepton nonuniversality parameter, which has been recently observed by LHCb in the $B^+ \rightarrow K^+ l^+ l^-$ process and has a 2.6σ discrepancy from the SM prediction in the dilepton invariant mass bin ($1 \leq q^2 \leq 6$) GeV². Analogously we would like to see whether it is possible to observe nonuniversality in the LFV decays. Hence, we define the ratios of branching ratios of various LFV decays as

$$R_{Kl}^{\mu e} = \frac{\text{Br}(\bar{B} \rightarrow \bar{K} \mu^- e^+)}{\text{Br}(\bar{B} \rightarrow \bar{K} l^+ l^-)}, \quad (44)$$

$$R_{Kl}^{\tau e} = \frac{\text{Br}(\bar{B} \rightarrow \bar{K} \tau^- e^+)}{\text{Br}(\bar{B} \rightarrow \bar{K} l^+ l^-)}, \quad (45)$$

$$R_{Kl}^{\tau \mu} = \frac{\text{Br}(\bar{B} \rightarrow \bar{K} \tau^- \mu^+)}{\text{Br}(\bar{B} \rightarrow \bar{K} l^+ l^-)}, \quad (46)$$

$$R_K^{\mu \mu} = \frac{\text{Br}(\bar{B} \rightarrow \bar{K} \mu^+ \mu^-)}{\text{Br}(\bar{B} \rightarrow \bar{K} e^+ e^-)}, \quad (47)$$

$$R_{Kl}^{\tau \tau} = \frac{\text{Br}(\bar{B} \rightarrow \bar{K} \tau^+ \tau^-)}{\text{Br}(\bar{B} \rightarrow \bar{K} l^+ l^-)}, \quad (48)$$

where $l = \mu, e$. Similarly, one can obtain the branching ratios and other physical observables in $B \rightarrow \pi l_i^- l_j^+$ processes by

incorporating the appropriate CKM matrix elements, form factors and the NP effective couplings. Recently, LHCb has measured the ratio of branching fractions of $B^+ \rightarrow \pi^+ \mu^+ \mu^-$ over $B^+ \rightarrow K^+ \mu^+ \mu^-$ processes [26], given as

$$\frac{\text{Br}(B^+ \rightarrow \pi^+ \mu^+ \mu^-)}{\text{Br}(B^+ \rightarrow K^+ \mu^+ \mu^-)} = 0.053 \pm 0.014(\text{stat}) \pm 0.001(\text{syst}). \quad (49)$$

In the same context, we also define the ratio of branching fractions of $B^+ \rightarrow \pi^+ l_i^- l_j^+$ and $B^+ \rightarrow K^+ l_i^- l_j^+$ LFV processes as

$$R_+^{l_i l_j} = \frac{\text{Br}(B^+ \rightarrow \pi^+ l_i^- l_j^+)}{\text{Br}(B^+ \rightarrow K^+ l_i^- l_j^+)}. \quad (50)$$

IV. NEW PHYSICS CONTRIBUTIONS DUE TO THE EXCHANGE OF VECTOR LEPTOQUARK

There are 10 different LQ multiplets under the $SU(3)_C \times SU(2)_L \times U(1)_Y$ SM gauge group [22], of these one half have scalar nature and the rest have vectorial nature under the Lorenz transformation. Vector LQs have spin 1 which exist in grand unified theories, $SO(10)$ including Pati-Salam color $SU(4)$ and larger gauge groups. The scalar and vector LQ multiplets are differ by their weak-hypercharge and fermion number. The strongest bounds on the vector LQs can be avoid by demanding chirality and diagonality of the coupling and diquark coupling have to be forbidden to evade proton decay. There are three relevant vector LQ multiplets, $(3, 3, 2/3)$, $(3, 1, 2/3)$, and $(\bar{3}, 2, 5/6)$ [23], out of which only $(3, 3, 2/3)$ leptoquark conserves both baryon and lepton numbers.

A. $Q=2/3$ vectors

There are two vector LQ multiplets $V^3(3, 3, 2/3)$ and $V^1(3, 1, 2/3)$, having fermion number zero and electric charge $Q = 2/3$. The interaction Lagrangian of the isotriplet state $V^{(3)}$ with the SM fermions is given by [23]

$$\mathcal{L}^{(3)} = g_L \bar{Q} \boldsymbol{\tau} \cdot V_\mu^{(3)} \gamma^\mu L + \text{H.c.}, \quad (51)$$

which conserves both lepton and baryon number and contributes new Wilson coefficients, $C_{V,A}^{\text{LQ}}$ as

$$C_V^{\text{LQ}} = -C_A^{\text{LQ}} = \frac{\pi}{\sqrt{2} G_F V_{tb} V_{ts}^* \alpha_{em}} \frac{(g_L)_{sl} (g_L)_{bl}^*}{M_{V^{(3)}}^2}. \quad (52)$$

Here, $Q(L)$ is the left-handed quark (lepton) doublet, g_L is the LQ coupling having left-handed quark current and $\boldsymbol{\tau}$ represents the Pauli matrices.

The Lagrangian for the isosinglet state, $V^{(1)}$, is given by

$$\mathcal{L}^{(1)} = (g_L \bar{Q} \gamma^\mu L + g_R \bar{d}_R \gamma^\mu l_R) V_\mu^{(1)} + \text{H.c.}, \quad (53)$$

where d_R and l_R are the right-handed down quark and lepton singlets, respectively, and g_R is the LQ coupling with down quarks and right-handed leptons. This LQ violates baryon number and has the coupling to both left- and right-handed fermions; i.e., it is a nonchiral LQ. In addition to $C_{V,A}$ new Wilson coefficients, these nonchiral LQ contributes scalar and pseudoscalar operators given by

$$C_V^{\text{NP}} = -C_A^{\text{NP}} = \frac{\pi}{\sqrt{2} G_F V_{tb} V_{ts}^* \alpha_{em}} \frac{(g_L)_{sl} (g_L)_{bl}^*}{M_{V^{(1)}}^2}, \quad (54a)$$

$$C_V^{\prime\text{NP}} = C_A^{\prime\text{NP}} = \frac{\pi}{\sqrt{2} G_F V_{tb} V_{ts}^* \alpha_{em}} \frac{(g_R)_{sl} (g_R)_{bl}^*}{M_{V^{(1)}}^2} \quad (54b)$$

$$-C_P^{\text{NP}} = C_S^{\text{NP}} = \frac{\sqrt{2} \pi}{G_F V_{tb} V_{ts}^* \alpha_{em}} \frac{(g_L)_{sl} (g_R)_{bl}^*}{M_{V^{(1)}}^2}, \quad (54c)$$

$$C_P^{\prime\text{NP}} = C_S^{\prime\text{NP}} = \frac{\sqrt{2} \pi}{G_F V_{tb} V_{ts}^* \alpha_{em}} \frac{(g_R)_{sl} (g_L)_{bl}^*}{M_{V^{(1)}}^2}. \quad (54d)$$

B. $Q=4/3$ vectors

The vector LQ with charge $Q = 4/3$ has one isospin doublet state $V^2(\bar{3}, 2, 5/6)$, whose coupling with fermion bilinear is given by [23]

$$\mathcal{L}^{(2)} = g_R \bar{Q}^C i \tau_2 V_\mu^{(2)} \gamma^\mu l_R + g_L \bar{d}_R^C \gamma^\mu \tilde{V}_\mu^{(2)\dagger} L + \text{H.c.} \quad (55)$$

This LQ also has both left-handed and right-handed lepton couplings and violates baryon number. Now performing the Fierz transformation, the additional Wilson coefficient contribution to the $b \rightarrow q l^- l^+$ process is

$$C_V^{\text{NP}} = C_A^{\text{NP}} = \frac{-\pi}{\sqrt{2} G_F V_{tb} V_{ts}^* \alpha_{em}} \frac{(g_R)_{bl} (g_R)_{sl}^*}{M_{V^{(2)}}^2}, \quad (56a)$$

$$-C_V^{\prime\text{NP}} = C_A^{\prime\text{NP}} = \frac{\pi}{\sqrt{2} G_F V_{tb} V_{ts}^* \alpha_{em}} \frac{(g_L)_{bl} (g_L)_{sl}^*}{M_{V^{(2)}}^2}, \quad (56b)$$

$$C_P^{\text{NP}} = C_S^{\text{NP}} = \frac{\sqrt{2} \pi}{G_F V_{tb} V_{ts}^* \alpha_{em}} \frac{(g_R)_{bl} (g_L)_{sl}^*}{M_{V^{(2)}}^2}, \quad (56c)$$

$$-C_P^{\prime\text{NP}} = C_S^{\prime\text{NP}} = \frac{\sqrt{2} \pi}{G_F V_{tb} V_{ts}^* \alpha_{em}} \frac{(g_L)_{bl} (g_R)_{sl}^*}{M_{V^{(2)}}^2}. \quad (56d)$$

V. CONSTRAINT ON THE LEPTOQUARK COUPLINGS

After having an idea about all possible new physics contributions to the SM, we now proceed to constrain the new Wilson coefficients by comparing the theoretical

and experimental branching ratios of various rare decay processes.

A. $B_{s,d} \rightarrow l^+ l^-$ processes

The rare leptonic $B_{s,d} \rightarrow \mu^+ \mu^-$ processes are mediated by the FCNC $b \rightarrow (s, d)$ transitions, and in the SM the branching ratios depend only on the Wilson coefficient C_A .

$$\text{Br}(B_q \rightarrow \mu^+ \mu^-) = \frac{G_F^2}{16\pi^3} \tau_{B_q} \alpha_{em}^2 f_{B_q}^2 M_{B_q} m_\mu^2 |V_{tb} V_{tq}^*|^2 |C_A^{\text{SM}}|^2 \sqrt{1 - \frac{4m_\mu^2}{M_{B_q}^2}} \times (|P|^2 + |S|^2), \quad (57)$$

where

$$P \equiv \frac{C_A^{\text{SM}} + C_A^{\text{LQ}} - C_A^{\text{LQ}}}{C_A^{\text{SM}}} + \frac{M_{B_q}^2}{2m_\mu} \left(\frac{m_b}{m_b + m_s} \right) \left(\frac{C_P^{\text{LQ}} - C_P^{\text{LQ}}}{C_A^{\text{SM}}} \right) \equiv |P| e^{i\phi_P},$$

$$S \equiv \sqrt{1 - \frac{4m_\mu^2}{M_{B_q}^2}} \frac{M_{B_q}^2}{2m_\mu} \left(\frac{m_b}{m_b + m_s} \right) \left(\frac{C_S^{\text{LQ}} - C_S^{\text{LQ}}}{C_A^{\text{SM}}} \right) \equiv |S| e^{i\phi_S}. \quad (58)$$

Here, the $C_A^{(\prime)\text{LQ}}$ and $C_{S,P}^{(\prime)\text{LQ}}$ Wilson coefficients are generated due to the vector LQ exchange and are negligible in the SM, which implies $P^{\text{SM}} = 1$ and $S^{\text{SM}} = 0$. The experimental result is related to the theoretical predictions as [28]

$$\text{Br}^{\text{th}}(B_q \rightarrow \mu^+ \mu^-) = \left[\frac{1 - y_q^2}{1 + A_{\Delta\Gamma} y_q} \right] \text{Br}^{\text{exp}}(B_q \rightarrow \mu^+ \mu^-), \quad (59)$$

where $y_q = \tau_{B_q} \Delta\Gamma_q/2$ and the observable $A_{\Delta\Gamma}$ is the mass eigenstate rate asymmetry equals to +1 in the SM. For calculational convenience, we define the parameter R_q as

$$R_q = \frac{\text{Br}^{\text{th}}(B_q \rightarrow \mu^+ \mu^-)}{\text{Br}^{\text{SM}}(B_q \rightarrow \mu^+ \mu^-)} = |P|^2 + |S|^2. \quad (60)$$

If we apply chirality on vector LQ, then the $C_{S,P}^{(\prime)\text{LQ}}$ Wilson coefficients will vanish and there will be additional contribution of only $C_{V,A}^{(\prime)\text{LQ}}$ Wilson coefficients to the SM. Hence, the R_q parameter can be given as [11,18]

$$R_q = \left| 1 + \frac{C_A^{\text{LQ}} - C_A^{\text{LQ}}}{C_A^{\text{SM}}} \right|^2 \equiv |1 + r e^{i\phi^{\text{NP}}}|^2, \quad (61)$$

where the parameters r and ϕ^{NP} are related to the new Wilson coefficients as

$$r e^{i\phi^{\text{NP}}} = \frac{C_A^{\text{LQ}} - C_A^{\text{LQ}}}{C_A^{\text{SM}}}. \quad (62)$$

In addition to the $C_{V,A}^{(\prime)}$ Wilson coefficients, the vector LQ also contributes scalar and pseudoscalar ($C_{S,P}^{(\prime)}$) Wilson coefficients to the SM. However, there is no additional contributions of tensor Wilson coefficients C_{T,T_5} due to the exchange of vector LQ.

The branching ratio of the $B_q \rightarrow \mu^+ \mu^-$ process in the LQ model is given by [27,28]

Now comparing the theoretical [29] branching ratios of the $B_q \rightarrow \mu^+ \mu^-$ processes with the 1σ range of experimental values [30], the constraint on r and ϕ^{NP} is computed for scalar LQ model in our previous work [11,18]. If we assume that both the scalar and vector LQs have same-order mass, $M_{\text{LQ}} = 1$ TeV, one can use the same constraint on r and ϕ^{NP} parameters to study the processes mediated via vector LQ. For $B_s \rightarrow \mu^+ \mu^-$ process, the constraints are found to be [11]

$$0 \leq r \leq 0.35, \quad \text{with} \quad \pi/2 \leq \phi^{\text{NP}} \leq 3\pi/2, \quad (63)$$

and for the $B_d \rightarrow \mu^+ \mu^-$ process [11],

$$0.5 \leq r \leq 1.3, \quad \text{for} \quad (0 \leq \phi^{\text{NP}} \leq \pi/2) \quad \text{or} \quad (3\pi/2 \leq \phi^{\text{NP}} \leq 2\pi). \quad (64)$$

Using Eqs. (52), (54a), and (54b), this can be translated to obtain the bounds on the LQ couplings (for $M_{\text{LQ}} = 1$ TeV) as

$$0 \leq |(g_L)_{s\mu} (g_L)_{b\mu}^*| \leq 2.3 \times 10^{-3}, \quad (65)$$

$$0.7 \times 10^{-3} \leq |(g_L)_{d\mu} (g_L)_{b\mu}^*| \leq 1.81 \times 10^{-3}. \quad (66)$$

Similarly, using the theoretical predictions [29] and the experimental upper limits [31,32] on $B_q \rightarrow e^+ e^- (\tau^+ \tau^-)$ processes, the constraints on the product of scalar LQ couplings are presented in Table I, which are found to be rather loose as the measured branching ratios of $B_{d,s} \rightarrow \tau^+ \tau^- (e^+ e^-)$ are not very precise.

TABLE I. Constraints on leptoquark couplings obtained from various leptonic $B_{s,d} \rightarrow l^+ l^-$ decays.

Decay process	Couplings involved	Upper bound of the couplings
$B_s \rightarrow e^\pm e^\mp$	$ (g_L)_{se}(g_L)_{be}^* $	< 11.8
$B_s \rightarrow \tau^\pm \tau^\mp$	$ (g_L)_{s\tau}(g_L)_{b\tau}^* $	< 0.4
$B_d \rightarrow e^\pm e^\mp$	$ (g_L)_{de}(g_L)_{be}^* $	< 8.0
$B_d \rightarrow \tau^\pm \tau^\mp$	$ (g_L)_{d\tau}(g_L)_{b\tau}^* $	< 0.593

For simplicity, we can neglect the NP contributions to the $C_{V,A}^{(\prime)LQ}$ Wilson coefficients, as the $C_{S,P}^{(\prime)LQ}$ Wilson coefficients are enhanced by the factor $M_{B_q}^2/m_l$. Now using Eqs. (58), (54c), (54d), and (60), the R_q parameter becomes

$$R_q = \frac{|C_S^{LQ} - C_S^{\prime LQ}|^2}{r_q^2} + \left| 1 - \frac{|C_S^{LQ} + C_S^{\prime LQ}|^2}{r_q} \right|, \quad (67)$$

where

$$r_q = \frac{2m_l(m_b + m_q)C_A^{SM}}{M_{B_q}^2}. \quad (68)$$

Now comparing the theoretical and experimental values of $B_q \rightarrow l^+ l^-$ decays, we calculate the allowed region of the $C_S^{LQ} \pm C_S^{\prime LQ}$ Wilson coefficients. If the Wilson coefficients are real, Eq. (67) will be a circle of radius $|r_q| \sqrt{R_q^{\text{expt}}}$ with center at $(C_S^{LQ} + C_S^{\prime LQ}, C_S^{LQ} - C_S^{\prime LQ}) = (r_q, 0)$. The left panel of Fig. 1 represents the constraint on real $C_S^{LQ} \pm C_S^{\prime LQ}$ Wilson coefficients from $B_s \rightarrow \mu^+ \mu^-$ process and the right panel is for complex Wilson coefficients. Similarly, in Fig. 2, we show the constraint on real (left panel) and complex (right panel) Wilson coefficients for $B_d \rightarrow \mu^+ \mu^-$ process. The allowed range of real Wilson coefficients from $B_s \rightarrow e^+ e^-$ (left panel) and $B_d \rightarrow e^+ e^-$ (right panel) processes are shown in Fig. 3. In Fig. 4, we present the constraint obtained from $B_s \rightarrow \tau^+ \tau^-$ (left panel) and $B_d \rightarrow \tau^+ \tau^-$ (right panel) processes. The allowed region of $C_S^{LQ} \pm C_S^{\prime LQ}$ real Wilson coefficients obtained from $B_q \rightarrow l^+ l^-$ processes are presented in

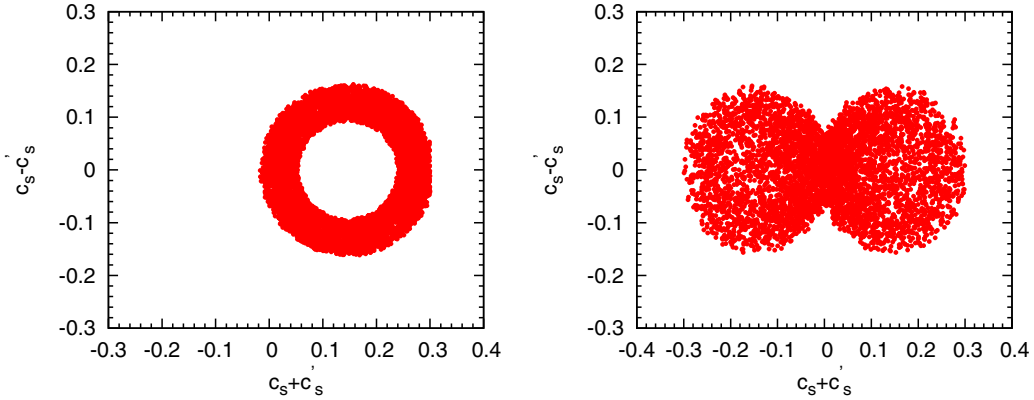


FIG. 1. Constraint on the combination of scalar Wilson coefficient from $B_s \rightarrow \mu^+ \mu^-$ process. The left panel is for real $C_S^{LQ} \pm C_S^{\prime LQ}$ Wilson coefficients and right panel is for complex Wilson coefficients.

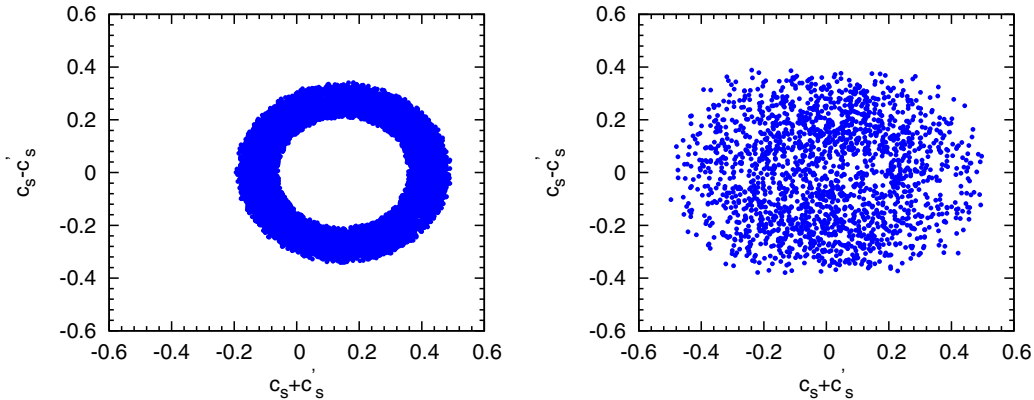


FIG. 2. Constraint on $C_S^{LQ} \pm C_S^{\prime LQ}$ Wilson coefficients from $B_d \rightarrow \mu^+ \mu^-$ process. The left panel is for real Wilson coefficients and right panel is for complex Wilson coefficients.

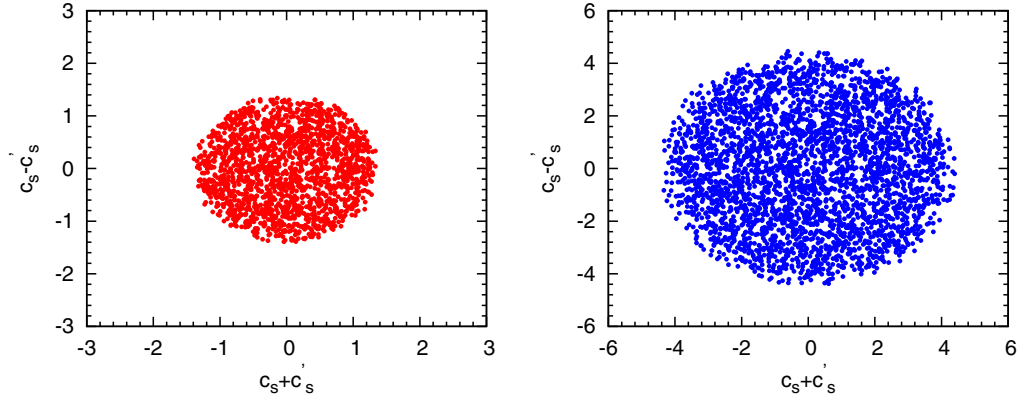


FIG. 3. The allowed region of $C_S^{\text{LQ}} - C_S^{\prime\text{LQ}}$ and $C_S^{\text{LQ}} + C_S^{\prime\text{LQ}}$ Wilson coefficients from $B_s \rightarrow e^+e^-$ (left panel) and $B_d \rightarrow e^+e^-$ (right panel) processes.

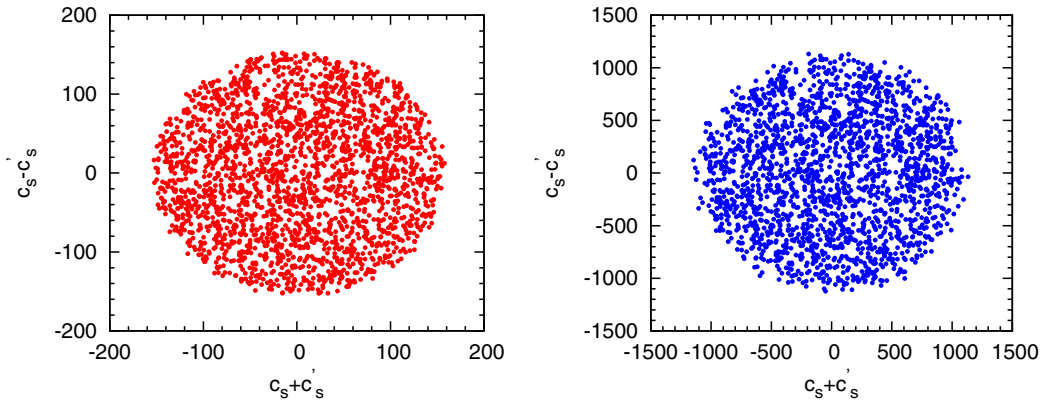


FIG. 4. The allowed region of $C_S^{\text{LQ}} - C_S^{\prime\text{LQ}}$ and $C_S^{\text{LQ}} + C_S^{\prime\text{LQ}}$ Wilson coefficients from $B_s \rightarrow \tau^+\tau^-$ (left panel) and $B_d \rightarrow \tau^+\tau^-$ (right panel) processes.

Table II. Now using the constrained Wilson coefficients, one can calculate the bound on the product of various LQ couplings from Eqs. (54c) and (54d).

B. $K_L \rightarrow \mu^+\mu^-(e^+e^-)$ process

The constraint on the product of various LQ couplings from the rare leptonic decays of K meson are discussed in this subsection. The rare $K_L \rightarrow \mu^+\mu^-$ decay mode has both the long and short distance contributions

TABLE II. Constraint on combinations of $C_S^{(\prime)\text{LQ}}$ Wilson coefficients from various leptonic $B_{s,d} \rightarrow l^+l^-$ decays.

Decay process	Bound on $C_S^{\text{LQ}} + C_S^{\prime\text{LQ}}$	Bound on $C_S^{\text{LQ}} - C_S^{\prime\text{LQ}}$
$B_s \rightarrow \mu^\pm\mu^\mp$	$0.0 \rightarrow 0.32$	$0.1 \rightarrow 0.18$
$B_s \rightarrow e^\pm e^\mp$	$-1.4 \rightarrow 1.4$	$-1.4 \rightarrow 1.4$
$B_s \rightarrow \tau^\pm\tau^\mp$	$-150 \rightarrow 150$	$-150 \rightarrow 150$
$B_d \rightarrow \mu^\pm\mu^\mp$	$-0.16 \rightarrow 0.44$	$0.2 \rightarrow 0.36$
$B_d \rightarrow e^\pm e^\mp$	$-4 \rightarrow 4$	$-4 \rightarrow 4$
$B_d \rightarrow \tau^\pm\tau^\mp$	$-1000 \rightarrow 1000$	$-1000 \rightarrow 1000$

and the dominant contribution comes from the long-distance two photon intermediates state $K_L \rightarrow \gamma^*\gamma^* \rightarrow \mu^+\mu^-$. Only the short distance (SD) part can be calculated reliably and the estimated branching ratio of the SD part is $\text{Br}(K_L \rightarrow \mu^+\mu^-)|_{\text{SD}} < 2.5 \times 10^{-9}$ [33]. In the SM, the effective Hamiltonian for the $K_L \rightarrow \mu^+\mu^-$ process is given by [34]

$$\mathcal{H}_{\text{eff}} = \frac{G_F}{\sqrt{2}} \frac{\alpha}{2\pi \sin^2 \theta_W} (\lambda_c Y_{NL} + \lambda_t Y(x_t)) (\bar{s} \gamma^\mu (1 - \gamma_5) d) \times (\bar{\mu} \gamma_\mu (1 - \gamma_5) \mu), \quad (69)$$

$$= \frac{G_F}{\sqrt{2}} \frac{\alpha}{2\pi} \lambda_u C_{\text{SM}}^K (\bar{s} \gamma^\mu (1 - \gamma_5) d) (\bar{\mu} \gamma_\mu (1 - \gamma_5) \mu), \quad (70)$$

where $\lambda_i = V_{id} V_{is}^*$, $x_t = m_t^2/M_W^2$ and $\sin^2 \theta_W = 0.23$ and C_{SM}^K is the SM Wilson coefficient given as

$$C_{\text{SM}}^K = \frac{\lambda_c Y_{NL} + \lambda_t Y(x_t)}{\sin^2 \theta_W \lambda_u}. \quad (71)$$

The functions Y_{NL} and $Y(x_t)$ are the contributions from charm and top quark, respectively, and the $Y(x_t)$ function in the next-to-leading order (NLO) is [35]

$$Y(x_t) = \eta_Y \frac{x_t}{8} \left(\frac{4-x_t}{1-x_t} + \frac{3x_t}{(1-x_t)^2} \ln x_t \right). \quad (72)$$

The branching ratio for the SD part of $K_L \rightarrow \mu^+ \mu^-$ process in the SM is given by

$$\begin{aligned} \text{Br}(K_L \rightarrow \mu^+ \mu^-)|_{\text{SD}} \\ = \tau_{K_L} \frac{G_F^2}{2\pi} |\lambda_u|^2 \sqrt{1 - \frac{4m_\mu^2}{M_K^2}} f_K^2 M_K m_\mu^2 |C_{\text{SM}}^K|^2. \end{aligned} \quad (73)$$

Now including the contribution of $V^{(1)}(3, 1, 2/3)$ leptoquark, the total branching ratio of $K_L \rightarrow \mu^+ \mu^-$ process is given by

$$\begin{aligned} \text{Br}(K_L \rightarrow \mu^+ \mu^-) = \frac{G_F^2}{8\pi^3} \tau_{K_L} \alpha_{em}^2 f_K^2 M_K m_\mu^2 |\lambda_u|^2 |C_{\text{SM}}^K|^2 \\ \times \sqrt{1 - \frac{4m_\mu^2}{M_K^2}} \times (|P_K|^2 + |S_K|^2), \end{aligned} \quad (74)$$

where

$$\begin{aligned} P_K &\equiv \frac{C_{\text{SM}}^K + C_A^{\text{LQ}} - C_S^{\text{LQ}}}{C_{\text{SM}}^K} + \frac{M_K^2}{2m_\mu} \left(\frac{m_s}{m_s + m_d} \right) \left(\frac{C_P^{\text{LQ}} - C_{P'}^{\text{LQ}}}{C_{\text{SM}}^K} \right), \\ S_K &\equiv \sqrt{1 - \frac{4m_\mu^2}{M_K^2}} \frac{M_K^2}{2m_\mu} \left(\frac{m_s}{m_s + m_d} \right) \left(\frac{C_S^{\text{LQ}} - C_S^{\text{LQ}}}{C_{\text{SM}}^K} \right). \end{aligned} \quad (75)$$

It should be noted that for $K_L \rightarrow \mu^+ \mu^-$ decay process, CP violation in $K - \bar{K}$ mixing is irrelevant and K_L can be treated as a pure CP -odd state. Therefore, we have to take into account the contributions of both K^0 and \bar{K}^0 amplitudes, which can be done by replacing the leptoquark couplings $(g_L)_{d\mu}(g_L)_{s\mu}^* \rightarrow \sqrt{2}\text{Re}[(g_L)_{d\mu}(g_L)_{s\mu}^*]$.

Thus, the new C_i^{LQ} coefficients arise due to the exchange of vector leptoquark and are defined as

$$C_A^{\text{LQ}} = -\frac{\pi}{G_F \alpha_{em} \lambda_u} \frac{\text{Re}[(g_L)_{d\mu}(g_L)_{s\mu}^*]}{M_{V^{(1)}}^2}, \quad (76a)$$

$$C_A^{\prime\text{LQ}} = -\frac{\pi}{G_F \alpha_{em} \lambda_u} \frac{\text{Re}[(g_R)_{d\mu}(g_R)_{s\mu}^*]}{M_{V^{(1)}}^2}, \quad (76b)$$

$$C_S^{\text{LQ}} = -C_P^{\text{LQ}} = \frac{\pi}{2G_F \alpha_{em} \lambda_u} \frac{\text{Re}[(g_L)_{d\mu}(g_R)_{s\mu}^*]}{M_{V^{(1)}}^2}, \quad (76c)$$

$$C_S^{\prime\text{LQ}} = C_P^{\prime\text{LQ}} = \frac{\pi}{2G_F \alpha_{em} \lambda_u} \frac{\text{Re}[(g_R)_{d\mu}(g_L)_{s\mu}^*]}{M_{V^{(1)}}^2}. \quad (76d)$$

In the presence of the $V^{(3)}(3, 3, 2/3)$ leptoquark, the branching is given by

$$\begin{aligned} \text{Br}(K_L \rightarrow \mu^+ \mu^-) = \frac{G_F^2}{8\pi^3} \tau_{K_L} \alpha_{em}^2 f_K^2 M_K m_\mu^2 |\lambda_u|^2 \sqrt{1 - \frac{4m_\mu^2}{M_K^2}} \\ \times \left| C_{\text{SM}}^K + \frac{C_A^{\text{LQ}}}{2} \right|^2. \end{aligned} \quad (77)$$

For muonic decay, the experimentally measured branching ratio is $\text{Br}(K_L \rightarrow \mu^+ \mu^-) = (6.84 \pm 0.11) \times 10^{-9}$ [13] and for the $K_L \rightarrow e^+ e^-$ process, the branching ratio is $\text{Br}(K_L \rightarrow e^+ e^-) = 9_{-4}^{+6} \times 10^{-12}$ [13]. If we apply chirality on the leptoquark, then only the $C_A^{(\prime)\text{LQ}}$ Wilson coefficients will contribute. Now comparing Eq. (74) with the experimental branching ratio of $K_L \rightarrow \mu^+ \mu^- (e^+ e^-)$ processes, the constraint on the leptoquark couplings for $M_{\text{LQ}} = 1$ TeV are given by

$$1.3 \times 10^{-3} \leq \text{Re}[(g_L)_{de}(g_L)_{se}^*] \leq 2.35 \times 10^{-3}, \quad (78)$$

$$1.4 \times 10^{-4} \leq \text{Re}[(g_L)_{d\mu}(g_L)_{s\mu}^*] \leq 1.5 \times 10^{-4}. \quad (79)$$

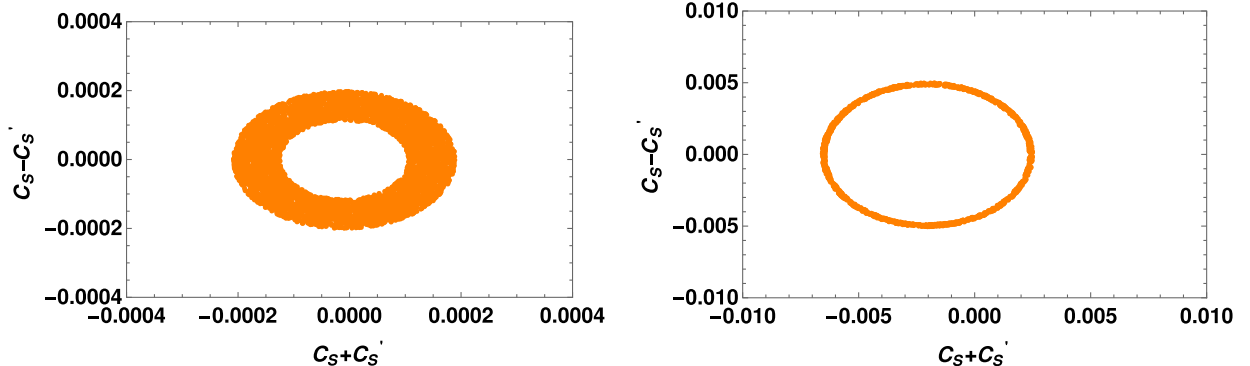


FIG. 5. The allowed region of $C_S^{\text{LQ}} \pm C_S^{\prime\text{LQ}}$ Wilson coefficients from $K_L \rightarrow e^+ e^-$ (left panel) and $K_L \rightarrow \mu^+ \mu^-$ (right panel) processes.

Now, by neglecting the C_A^{LQ} coefficients, the constraints on $(C_S^{\text{LQ}} \pm C_S^{\prime\text{LQ}})$ Wilson coefficients from $K_L \rightarrow e^+e^-$ (left panel) and $K_L \rightarrow \mu^+\mu^-$ (right panel) are shown in Fig. 5. From the figure the allowed regions of LQ couplings for $K_L \rightarrow e^+e^-$ process are given by

$$-2 \times 10^{-4} \leq C_S^{\text{LQ}} + C_S^{\prime\text{LQ}} \leq 2 \times 10^{-4}, \quad (80)$$

$$1.25 \times 10^{-4} \leq C_S^{\text{LQ}} - C_S^{\prime\text{LQ}} \leq 2 \times 10^{-4}, \quad (81)$$

and for $K_L \rightarrow \mu^+\mu^-$ process,

$$-6 \times 10^{-3} \leq C_S^{\text{LQ}} + C_S^{\prime\text{LQ}} \leq 3 \times 10^{-3}, \quad (82)$$

$$5 \times 10^{-5} \leq C_S^{\text{LQ}} - C_S^{\prime\text{LQ}} \leq 5.6 \times 10^{-3}. \quad (83)$$

C. $\tau^- \rightarrow \mu^- \gamma$ process

In this subsection, we compute the constraint on $V_\mu^1(3, 1, 2/3)$ vector LQ couplings from the charged lepton flavor violating processes like $\tau^- \rightarrow l^- \gamma$, where $l = \mu, e$. These radiative decays provide an important testing ground for many new physics beyond the SM. The similar analysis in the context of scalar LQs can be found in the literature [24]. In Ref. [36], the authors have given the general loop formulas for the radiative decay modes. The effective Hamiltonian for the $\tau^- \rightarrow \mu^- \gamma$ process is given by

$$\mathcal{H}_{\text{eff}} = e(C_L \bar{\mu}_R \sigma^{\mu\nu} F_{\mu\nu} \tau_L + C_R \bar{\mu}_L \sigma^{\mu\nu} F_{\mu\nu} \tau_R), \quad (84)$$

where $\sigma^{\mu\nu}$ is the photon field strength tensor and the Wilson coefficients $C_{L,R}$ are expressed as

$$\begin{aligned} C_L = & \frac{N_c}{16\pi^2 M_{V(1)}^2} \left(-\frac{1}{3} [(g_L)_{b\tau} (g_L)_{b\mu}^* f_2(x_b) + (g_R)_{b\tau} (g_R)_{b\mu}^* f_1(x_b) + (g_L)_{b\tau} (g_R)_{b\mu}^* f_3(x_b) + (g_R)_{b\tau} (g_L)_{b\mu}^* f_4(x_b)] \right. \\ & \left. + \frac{2}{3} [(g_L)_{b\tau} (g_L)_{b\mu}^* \bar{f}_2(x_b) + (g_R)_{b\tau} (g_R)_{b\mu}^* \bar{f}_1(x_b) + (g_L)_{b\tau} (g_R)_{b\mu}^* f_3(x_b) + (g_R)_{b\tau} (g_L)_{b\mu}^* f_4(x_b)] \right) \\ & + \frac{N_c}{16\pi^2 M_{V(3)}^2} (g_L)_{b\tau} (g_L)_{b\mu}^* \left[-\frac{1}{6} f_2^{(3)}(x_b) + \frac{1}{3} \bar{f}_2^{(3)}(x_b) \right], \end{aligned} \quad (85)$$

$$\begin{aligned} C_R = & \frac{N_c}{16\pi^2 M_{V(1)}^2} \left(-\frac{1}{3} [(g_L)_{b\tau} (g_L)_{b\mu}^* f_1(x_b) + (g_R)_{b\tau} (g_R)_{b\mu}^* f_2(x_b) + (g_L)_{b\tau} (g_R)_{b\mu}^* f_4(x_b) + (g_R)_{b\tau} (g_L)_{b\mu}^* f_3(x_b)] \right. \\ & \left. + \frac{2}{3} [(g_L)_{b\tau} (g_L)_{b\mu}^* \bar{f}_1(x_b) + (g_R)_{b\tau} (g_R)_{b\mu}^* \bar{f}_2(x_b) + (g_L)_{b\tau} (g_R)_{b\mu}^* \bar{f}_4(x_b) + (g_R)_{b\tau} (g_L)_{b\mu}^* \bar{f}_3(x_b)] \right) \\ & + \frac{N_c}{16\pi^2 M_{V(3)}^2} (g_L)_{b\tau} (g_L)_{b\mu}^* \left[-\frac{1}{6} f_1^{(3)}(x_b) + \frac{1}{3} \bar{f}_1^{(3)}(x_b) \right]. \end{aligned} \quad (86)$$

Here, $N_c = 3$ is the color factor, $x_b = m_b^2/M_{\text{LQ}}^2$ (where $M_{\text{LQ}} = M_{V(1)}$ or $M_{V(3)}$), and the loop functions are given as [36]

$$f_1(x_b) = m_\tau \left[\frac{-5x_b^3 + 9x_b^2 - 30x_b + 8}{12(x_b - 1)^3} + \frac{3x_b^2 \ln x_b}{2(x_b - 1)^4} \right], \quad (87a)$$

$$f_2(x_b) = m_\mu \left[\frac{-5x_b^3 + 9x_b^2 - 30x_b + 8}{12(x_b - 1)^3} + \frac{3x_b^2 \ln x_b}{2(x_b - 1)^4} \right], \quad (87b)$$

$$f_3(x_b) = m_b \left[\frac{x_b^2 + x_b + 4}{2(x_b - 1)^2} - \frac{3x_b \ln x_b}{(x_b - 1)^3} \right], \quad (87c)$$

$$f_4(x_b) = -\frac{m_\tau m_\mu m_b}{m_{V(1)}^2} \left[\frac{-2x_b^2 + 7x_b - 11}{6(x_b - 1)^3} + \frac{\ln x_b}{(x_b - 1)^4} \right], \quad (87d)$$

$$\bar{f}_1(x_b) = m_\tau \left[\frac{-4x_b^3 + 45x_b^2 - 33x_b + 10}{12(x_b - 1)^3} - \frac{3x_b^3 \ln x_b}{2(x_b - 1)^4} \right], \quad (87e)$$

$$\bar{f}_2(x_b) = m_\mu \left[\frac{-4x_b^3 + 45x_b^2 - 33x_b + 10}{12(x_b - 1)^3} - \frac{3x_b^3 \ln x_b}{2(x_b - 1)^4} \right], \quad (87f)$$

$$\bar{f}_3(x_b) = m_b \left[\frac{x_b^2 - 11x_b + 4}{2(x_b - 1)^2} + \frac{3x_b^2 \ln x_b}{(x_b - 1)^3} \right], \quad (87g)$$

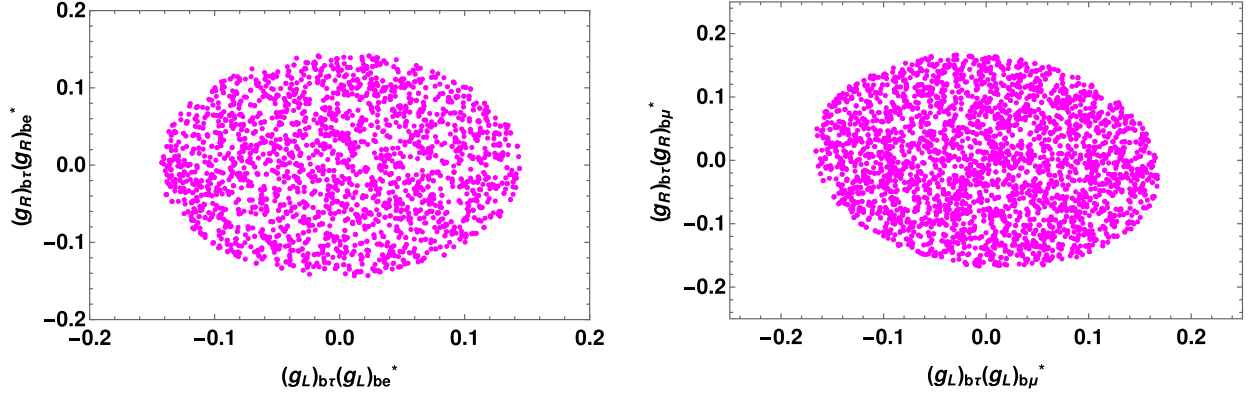


FIG. 6. The constraint on $(g_L)_{b\tau_i}(g_L)_{b\tau_j}^*$ and $(g_R)_{b\tau_i}(g_R)_{b\tau_j}^*$ leptoquark couplings from $\tau^- \rightarrow e^- \gamma$ (left panel) and $\tau^- \rightarrow \mu^- \gamma$ (right panel) processes.

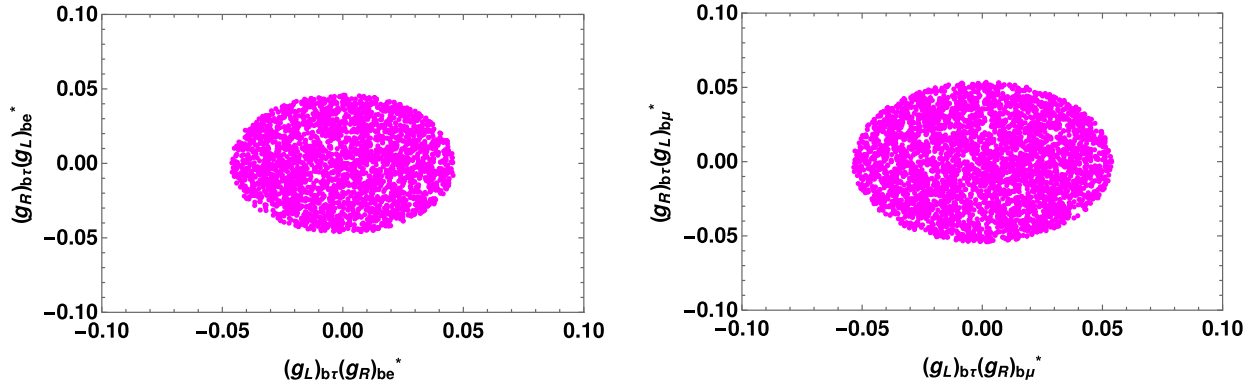


FIG. 7. The constraint on $(g_L)_{b\tau_i}(g_R)_{b\tau_j}^*$ and $(g_R)_{b\tau_i}(g_L)_{b\tau_j}^*$ leptoquark couplings from $\tau^- \rightarrow e^- \gamma$ (left panel) and $\tau^- \rightarrow \mu^- \gamma$ (right panel) processes.

$$\begin{aligned} \bar{f}_4(x_b) = & \frac{m_\tau m_\mu m_b}{m_{V(1)}^2} \left[\frac{x_b^2 - 5x_b - 6 - 6x_b(1+x_b) \ln x_b}{6(x_b - 1)^3} \right. \\ & \left. + \frac{x_b^3 \ln x_b}{(x_b - 1)^4} \right]. \end{aligned} \quad (87h)$$

The branching ratio of the $\tau^- \rightarrow \mu^- \gamma$ process is given by

$$\text{Br}(\tau^- \rightarrow \mu^- \gamma) = \frac{\tau_\tau (m_\tau^2 - m_\mu^2)^3}{16\pi m_\tau^3} [|C_L|^2 + |C_R|^2]. \quad (88)$$

This expression can be applied to study other LFV radiative decays like, $\tau^- \rightarrow e^- \gamma$ and $\mu^- \rightarrow e^- \gamma$. The current upper bounds on the branching ratios of $\tau^- \rightarrow \mu^- (e^-) \gamma$ is given by [13]

$$\begin{aligned} \text{Br}(\tau^- \rightarrow \mu^- \gamma) & < 4.4 \times 10^{-8}, \\ \text{Br}(\tau^- \rightarrow e^- \gamma) & < 3.3 \times 10^{-8}. \end{aligned} \quad (89)$$

Comparing Eq. (88) with the current experimental bounds (89), the allowed regions of $(g_{L(R)})_{b\tau_i}(g_{L(R)})_{b\tau_j}^*$ couplings

from $\tau^- \rightarrow e^- \gamma$ (left panel) and $\tau^- \rightarrow \mu^- \gamma$ (right panel) are shown in Fig. 6, and the constraints on the $(g_{L(R)})_{b\tau_i}(g_{L(R)})_{b\tau_j}^*$ leptoquark couplings from $\tau^- \rightarrow e^- \gamma$ (left panel) and $\tau^- \rightarrow \mu^- \gamma$ (right panel) are presented in Fig. 7. The numerical values of the constraints on leptoquark couplings are given in Table III. These bounds are rather weak in comparison to $B_{s,d} \rightarrow \mu^+ \mu^-$ processes and they also involve the coupling only to b quark in both the LQ coupling parameters.

VI. NUMERICAL ANALYSIS OF LFV DECAYS

After having detailed knowledge about the observables and the bound on new Wilson coefficients, we now proceed to a numerical analysis of LFV decays in the LQ model. Though LFV decays are extremely rare in the SM due to loop suppression and the presence of tiny neutrino mass in the loop, still they can occur at tree level and are expected to have significantly large branching ratios in the LQ model. There will be no contributions from SM Wilson coefficients in the LFV decays of the B meson.

In the presence of LQ, the modified helicity amplitudes are given as

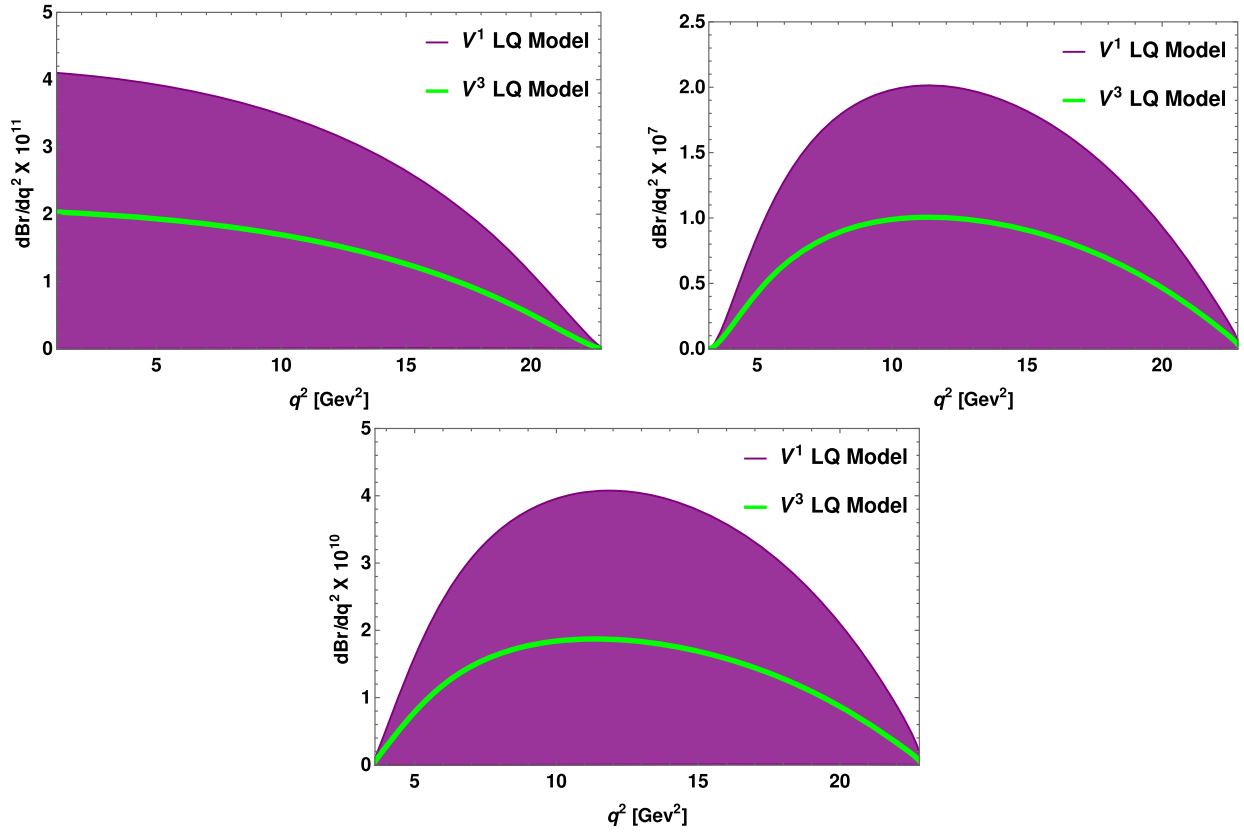


FIG. 8. The variation of branching ratios of $B^+ \rightarrow K^+ \mu^- e^+$ (top left panel), $B^+ \rightarrow K^+ \tau^- e^+$ (top right panel) and $B^+ \rightarrow K^+ \tau^- \mu^+$ (bottom panel) processes (in units of GeV^{-2}) in the $V^{1,3}$ vector leptoquark model. Here purple bands represent the contribution from V^1 leptoquark model and green solid lines are for V^3 leptoquark.

$$H_V^{0\text{LQ}} = \sqrt{\frac{\lambda}{q^2}} (C_V^{\text{LQ}} + C_V^{\prime\text{LQ}}) f_+(q^2), \quad (90)$$

$$H_S^{\text{LQ}} = \frac{M_B^2 - M_K^2}{m_b} (C_S^{\text{LQ}} + C_S^{\prime\text{LQ}}) f_0(q^2), \quad (94)$$

$$H_V^{\text{LQ}} = \frac{M_B^2 - M_K^2}{\sqrt{q^2}} (C_V^{\text{LQ}} + C_V^{\prime\text{LQ}}) f_0(q^2), \quad (91)$$

$$H_P^{\text{LQ}} = \frac{M_B^2 - M_K^2}{m_b} (C_P^{\text{LQ}} + C_P^{\prime\text{LQ}}) f_0(q^2). \quad (95)$$

$$H_A^{0\text{LQ}} = \sqrt{\frac{\lambda}{q^2}} (C_A^{\text{LQ}} + C_A^{\prime\text{LQ}}) f_+(q^2), \quad (92)$$

$$H_A^{\text{LQ}} = \frac{M_B^2 - M_K^2}{\sqrt{q^2}} (C_A^{\text{LQ}} + C_A^{\prime\text{LQ}}) f_0(q^2), \quad (93)$$

TABLE III. Constraints on leptoquark couplings obtained from the $\tau^- \rightarrow l^- \gamma$ processes.

Couplings involved	$\tau^- \rightarrow e^- \gamma$ process	$\tau^- \rightarrow \mu^- \gamma$ process
$(g_L)_{b\tau} (g_L)_{bl}^*$	$-0.14 \rightarrow 0.14$	$-0.16 \rightarrow 0.16$
$(g_R)_{b\tau} (g_R)_{bl}^*$	$-0.14 \rightarrow 0.14$	$-0.16 \rightarrow 0.16$
$(g_L)_{b\tau} (g_R)_{bl}^*$	$-0.04 \rightarrow 0.04$	$-0.05 \rightarrow 0.05$
$(g_R)_{b\tau} (g_L)_{bl}^*$	$-0.04 \rightarrow 0.04$	$-0.05 \rightarrow 0.05$

For numerical analysis, we have taken the particle masses and life times of B_q mesons from [13]. The form factors ($f_{0,+,\tau}$) for the kaon and pion are taken from [37] and [38], respectively. In order to compute the required LQ couplings, we use the values of the couplings extracted from $B_{s,d} \rightarrow l^+ l^-$, as given in Tables I and II. Although the bounds obtained from $K_L \rightarrow l^+ l^-$ processes (79) are little stronger than the bounds obtained from $B_{s,d} \rightarrow l^+ l^-$, only the Real part of the couplings can be constrained there. Therefore, in our analysis, we consider the constraints from Tables I and II as basis values and assume that the LQ couplings between different generation of quark and lepton follow the simple scaling law, i.e., $(g_{L(R)})_{ij} = (m_i/m_j)^{1/2} (g_{L(R)})_{ii}$ with $j > i$. This ansatz was taken from Ref. [39], which can explain the decay width of radiative LFV $\mu \rightarrow e \gamma$ decay. Now using the constrained LQ parameter space,

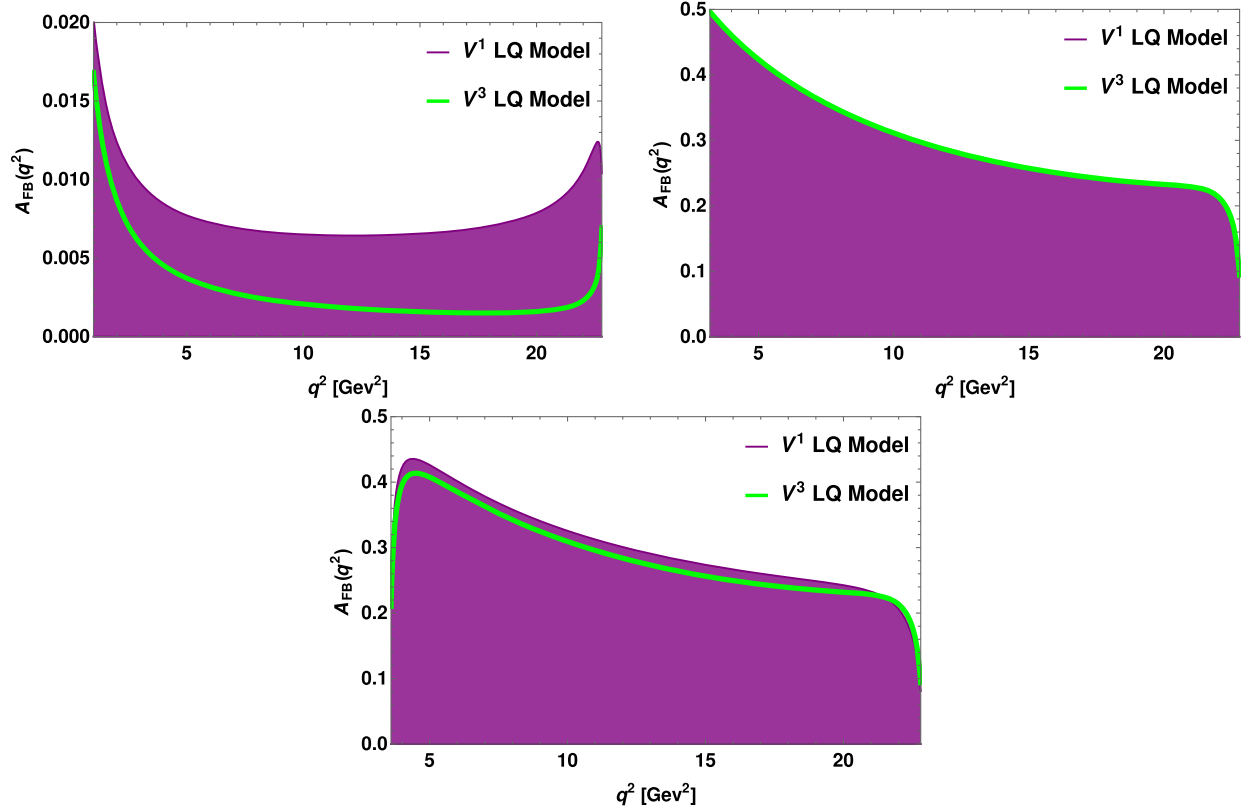


FIG. 9. The variation of forward-backward asymmetries of $B^+ \rightarrow K^+ \mu^- e^+$ (top left panel), $B^+ \rightarrow K^+ \tau^- e^+$ (top right panel) and $B^+ \rightarrow K^+ \tau^- \mu^+$ (bottom panel) processes in the leptoquark model.

we calculate the branching ratios, forward-backward asymmetries and lepton nonuniversality in $B \rightarrow K(\pi) l_i^- l_j^+$ processes. In Fig. 8, we show the variation of branching ratios of $B^+ \rightarrow K^+ \mu^- e^+$ (top left panel), $B^+ \rightarrow K^+ \tau^- e^+$ (top right panel) and $B^+ \rightarrow K^+ \tau^- \mu^+$ (bottom panel) processes with respect to q^2 in both $V^{1,3}$ leptoquark model. Here the purple bands represent the predictions in the V^1 vector LQ model and green solid lines are for V^3 leptoquark. The predicted branching ratios of $B^+ \rightarrow K^+ l_i^- l_j^+$ processes in both the LQ model are presented in Table IV. The plot for forward-backward asymmetries of $B^+ \rightarrow K^+ \mu^- e^+$ (top left panel), $B^+ \rightarrow K^+ \tau^- e^+$ (top right panel) and $B^+ \rightarrow K^+ \tau^- \mu^+$ (bottom

panel) processes in the LQ model are given in Fig. 9. Figure 10 shows the q^2 variation of $R_{Ke}^{\mu e}$ (top right panel), $R_{Ke}^{\tau e}$ (bottom left panel) and $R_{K\mu}^{\tau\mu}$ (bottom right panel) parameters in the high q^2 region. The variation of $R_{K\mu}^{\mu e}$ (top right panel), $R_{K\mu}^{\tau e}$ (bottom left panel) and $R_{K\mu}^{\tau\mu}$ (bottom right panel) observables are presented in Fig. 11. The variation of $R_{Ke}^{\mu e}$ and $R_{K\mu}^{\mu e}$ parameters in low $q^2 \in [1, 6]$ region are also shown in the top left panel of Fig. 10 and Fig. 11, respectively. The integrated values of forward-backward asymmetries and lepton nonuniversality parameters such as $R_K^{l_i l_j}$, $R_{Ke}^{l_i l_j}$, $R_{K\mu}^{l_i l_j}$ are given in Table V. In Fig. 12 we show the plot for lepton nonuniversality parameters $R_K^{\mu\mu}$ in low q^2 (left panel)

TABLE IV. The predicted branching ratios of $B^+ \rightarrow K^+(\pi^+) l_i^- l_j^+$ processes in the $V^{1,3}$ vector leptoquark model.

Decay process	Values in V^1 LQ model	Values in V^3 LQ model	Exp. upper limit [13]
$B^+ \rightarrow K^+ \mu^- e^+$	$(0.009-6.16) \times 10^{-10}$	$< 2.98 \times 10^{-10}$	$< 9.1 \times 10^{-8}$
$B^+ \rightarrow K^+ \tau^- e^+$	$(0.118-1.882) \times 10^{-10}$	$< 7.12 \times 10^{-11}$	$< 4.3 \times 10^{-5}$
$B^+ \rightarrow K^+ \tau^- \mu^+$	$(0.0064-5.58) \times 10^{-9}$	$< 2.52 \times 10^{-9}$	$< 4.5 \times 10^{-5}$
$B^+ \rightarrow \pi^+ \mu^- e^+$	$(0.48-3.23) \times 10^{-10}$	$< 1.6 \times 10^{-10}$	$< 6.4 \times 10^{-3}$
$B^+ \rightarrow \pi^+ \tau^- e^+$	$5.23 \times 10^{-12}-1.51 \times 10^{-6}$	$< 7.55 \times 10^{-7}$	$< 7.4 \times 10^{-5}$
$B^+ \rightarrow \pi^+ \tau^- \mu^+$	$(0.41-2.99) \times 10^{-9}$	$< 1.46 \times 10^{-9}$	$< 6.2 \times 10^{-5}$

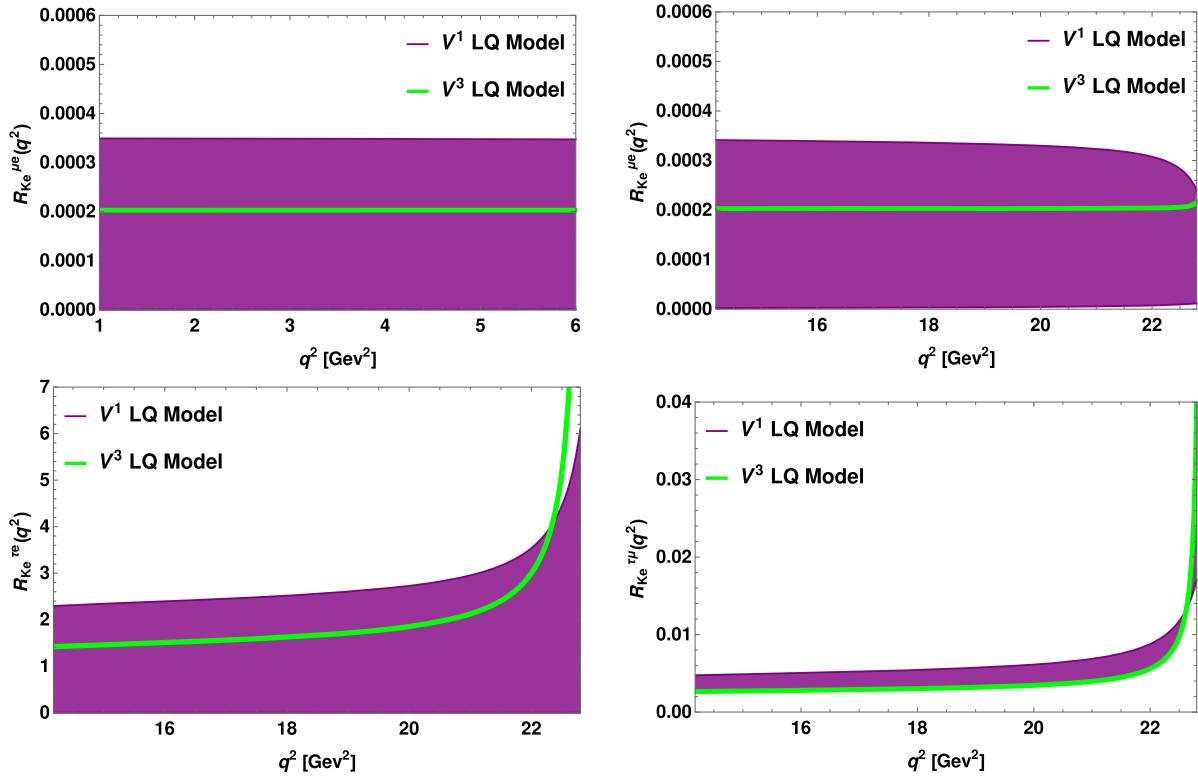


FIG. 10. The plots for lepton nonuniversality parameters, $R_{K_e}^{\mu e}$ (top right panel), $R_{K_e}^{\tau e}$ (bottom left panel) and $R_{K_e}^{\tau \mu}$ (bottom right panel) in high q^2 region. Here the top left panel shows the nonuniversality $R_{K_e}^{\mu e}$ in low $q^2 \in [1, 6]$ region.

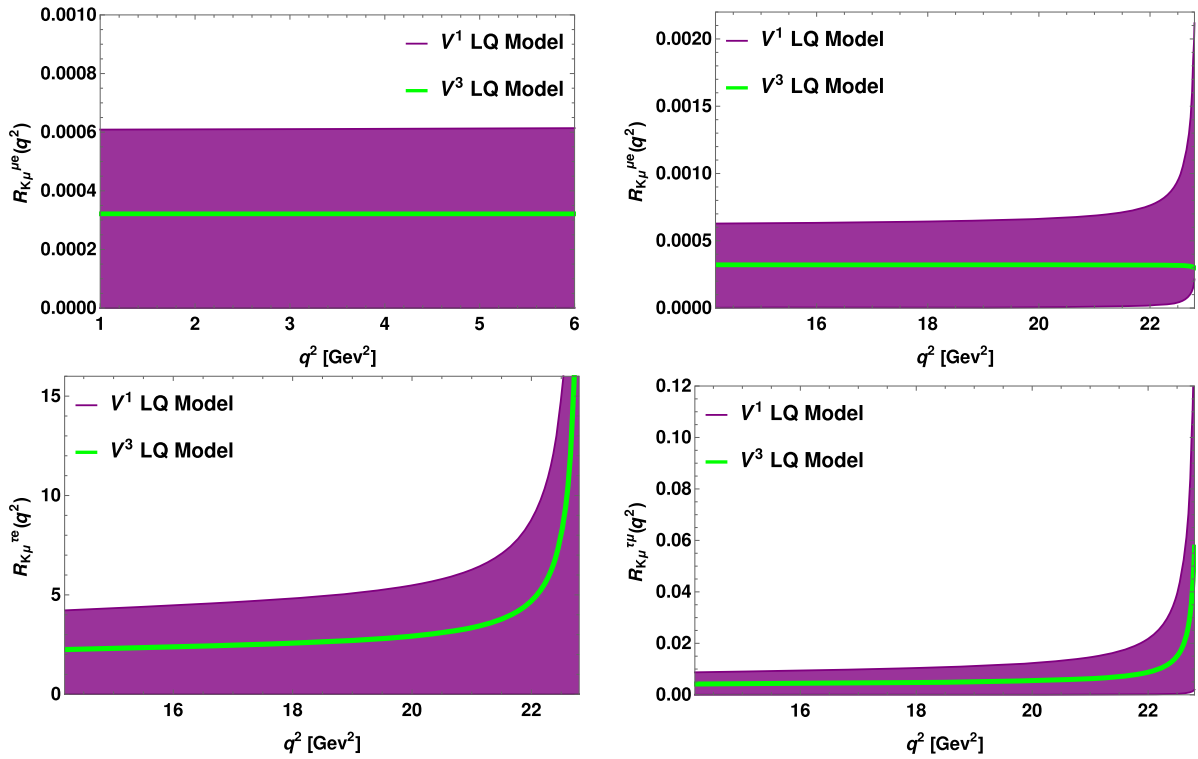


FIG. 11. The plots for lepton nonuniversality parameters, $R_{K_\mu}^{\mu e}$ (top right panel), $R_{K_\mu}^{\tau e}$ (bottom left panel) and $R_{K_\mu}^{\tau \mu}$ (bottom right panel) in high q^2 region. Here the top left panel shows the nonuniversality $R_{K_\mu}^{\mu e}$ in low $q^2 \in [1, 6]$ region.

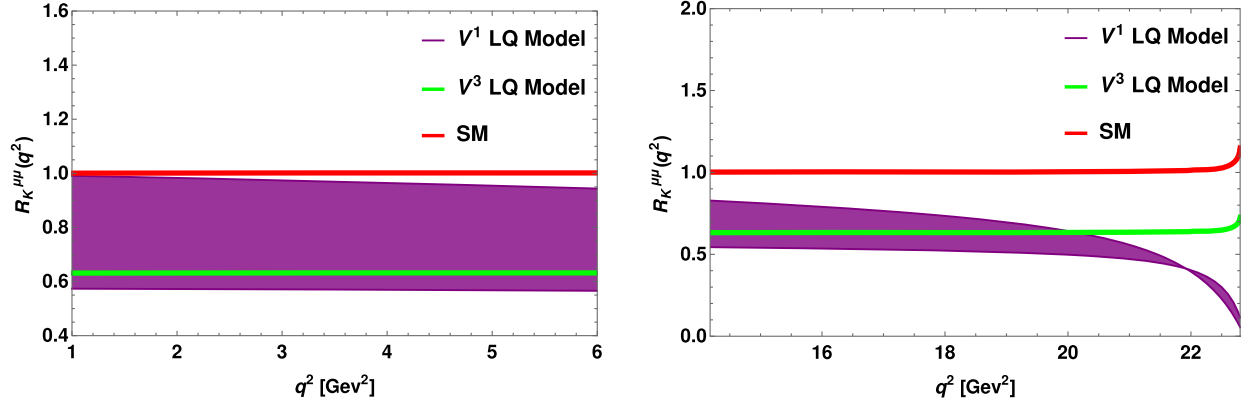


FIG. 12. The variation of lepton nonuniversality parameter $R_K^{\mu\mu}$ for low $q^2 \in [1, 6]$ (left panel) and high q^2 (right panel) regimes.

and high q^2 (right panel) and the predicted values are presented in Table V. Here the solid red lines denote the SM contributions and integrated values in the SM are given by

$$\begin{aligned} R_K^{\mu\mu}|_{q^2 \in [1,6]} &= 1.001, & R_K^{\mu\mu}|_{q^2 \geq 14.18} &= 1.003, \\ R_{Ke}^{\tau\tau} &= 1.144, & R_{K\mu}^{\tau\tau} &= 1.14. \end{aligned} \quad (96)$$

Analogously, we show the variation of the branching ratios of LFV $B^+ \rightarrow \pi^+ \mu^- e^+$ (top left panel), $B^+ \rightarrow \pi^+ \tau^- e^+$ (top right panel) and $B^+ \rightarrow \pi^+ \tau^- \mu^+$ (bottom panel) decay processes with respect to q^2 in Fig. 13 and the predicted branching ratios are given in Table IV. Fig. 14 shows the variation of forward-backward asymmetries in $B^+ \rightarrow \pi^+ \mu^- e^+$ (top left panel),

TABLE V. The predicted values of forward-backward asymmetries and lepton nonuniversality parameters in $B^+ \rightarrow K^+ l^- l_j^+$ process in the $V^{1,3}$ vector leptoquark model. Also the predicted values of $R_K^{\mu\mu}$, $R_{Ke}^{l_j l_j}$, $R_{K\mu}^{l_j l_j}$ parameters for muonic (electronic) processes in low $q^2 \in [1, 6]$ region.

Observables	Values in V^1 LQ model	Values in V^3 LQ model
$\langle A_{FB}^{K\mu e} \rangle$	7.65×10^{-3}	2.82×10^{-3}
$\langle A_{FB}^{K\tau e} \rangle$	0.285	0.285
$\langle A_{FB}^{K\tau\mu} \rangle$	$(0.039-0.105) \times 10^{-3}$	4.8×10^{-3}
$\langle R_{Ke}^{\mu e} \rangle _{q^2 \in [1,6]}$	$(0.0038-3.5) \times 10^{-4}$	2.03×10^{-4}
$\langle R_{Ke}^{\tau e} \rangle$	$(0.033-3.36) \times 10^{-4}$	2.04×10^{-4}
$\langle R_{Ke}^{\tau\tau} \rangle$	$0.526 \times 10^{-4}-2.52$	1.63
$\langle R_{K\mu}^{\tau\mu} \rangle$	$(0.285-5.45) \times 10^{-3}$	3.04×10^{-3}
$\langle R_{K\mu}^{\mu e} \rangle _{q^2 \in [1,6]}$	$(0.0039-6.1) \times 10^{-4}$	3.2×10^{-4}
$\langle R_{K\mu}^{\tau e} \rangle$	$(0.0454-6.44) \times 10^{-4}$	3.3×10^{-4}
$\langle R_{K\mu}^{\tau\tau} \rangle$	$0.72 \times 10^{-4}-4.83$	2.58
$\langle R_{K\mu}^{\tau\mu} \rangle$	$(0.039-0.1) \times 10^{-3}$	4.8×10^{-3}
$\langle R_K^{\mu\mu} \rangle _{q^2 \in [1,6]}$	0.57-0.9688	0.63
$\langle R_K^{\mu\mu} \rangle$	0.521-0.73	0.64

$B^+ \rightarrow \pi^+ \tau^- e^+$ (top right panel) and $B^+ \rightarrow \pi^+ \tau^- \mu^+$ (bottom panel) processes. The lepton nonuniversality parameters $R_{\pi\mu}^{\mu e}$ (top right panel), $R_{\pi\mu}^{\tau e}$ (bottom left panel) and $R_{\pi\mu}^{\tau\mu}$ (bottom right panel) are presented in Fig. 15. Also, we present the behavior of $R_{\pi\mu}^{\mu e}$ parameter (top left panel) in the region $1 \leq q^2 \leq 6 \text{ GeV}^2$. In Table VI, we present the predicted values of forward-backward asymmetries and lepton nonuniversality parameters. The nonuniversality predictions of the $B \rightarrow \pi l^+ l^-$ processes in the SM are

$$\begin{aligned} R_{\pi}^{\mu\mu}|_{q^2 \in [1,6]} &= 1.001, & R_{\pi}^{\mu\mu}|_{q^2 \geq 14.18} &= 1.003, \\ R_{\pi e}^{\tau\tau} &= 1.149, & R_{\pi\mu}^{\tau\tau} &= 1.146, \end{aligned} \quad (97)$$

and the values for the parameter $R_{\pi}^{\mu\mu}$ in the LQ model are listed in Table VI.

The predicted values of $R_+^{l_j l_j}$ in $V^{1,3}$ LQ model, respectively, are

$$R_+^{\mu e}|_{V^1 \text{LQ}} = 0.525-53.34, \quad R_+^{\mu e}|_{V^3 \text{LQ}} = 0.536, \quad (98)$$

$$R_+^{\tau\mu}|_{V^1 \text{LQ}} = 0.536-64.1, \quad R_+^{\tau\mu}|_{V^3 \text{LQ}} = 0.578, \quad (99)$$

$$R_+^{\tau e}|_{V^1 \text{LQ}} = 0.443-0.56, \quad R_+^{\tau e}|_{V^3 \text{LQ}} = 0.56. \quad (100)$$

VII. $(g-2)_\mu$

The recent experimental measurement [40] of the anomalous magnetic moment of muon, i.e., $(g-2)_\mu$ has about 3σ discrepancies from the SM prediction and has set off a flurry of excitement amongst theorists. The experimental result of anomalous magnetic moment of muon is given by [41]

$$a_\mu^{\text{exp}} = 116592080(63) \times 10^{-11}, \quad (101)$$

which when compared to the SM value

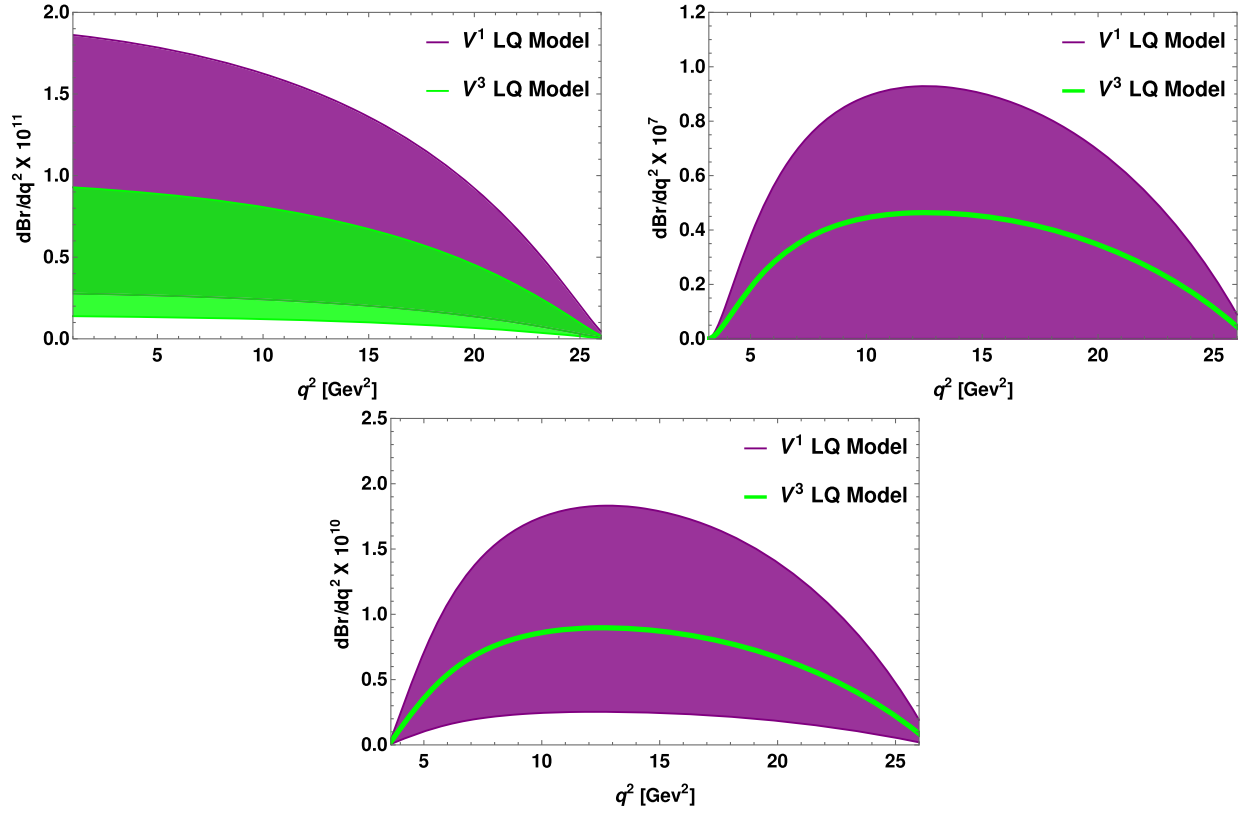


FIG. 13. The q^2 variation of branching ratios of $B^+ \rightarrow \pi^+ \mu^- e^+$ (top left panel), $B^+ \rightarrow \pi^+ \tau^- e^+$ (top right panel) and $B^+ \rightarrow \pi^+ \tau^- \mu^+$ (bottom panel) processes in the $V^{1,3}$ vector leptoquark model.

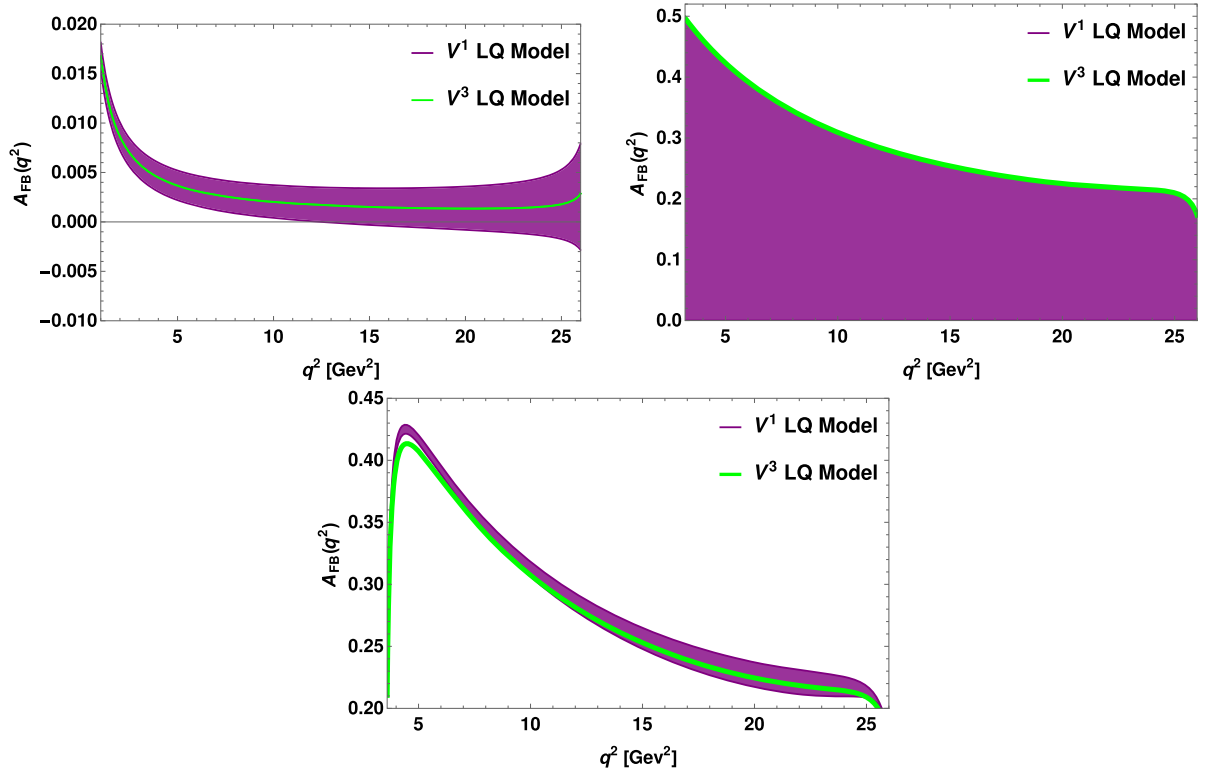


FIG. 14. The variations of forward-backward asymmetries of $B^+ \rightarrow \pi^+ \mu^- e^+$ (left panel), $B^+ \rightarrow \pi^+ \tau^- e^+$ (middle panel) and $B^+ \rightarrow \pi^+ \tau^- \mu^+$ (right panel) processes in leptoquark model.

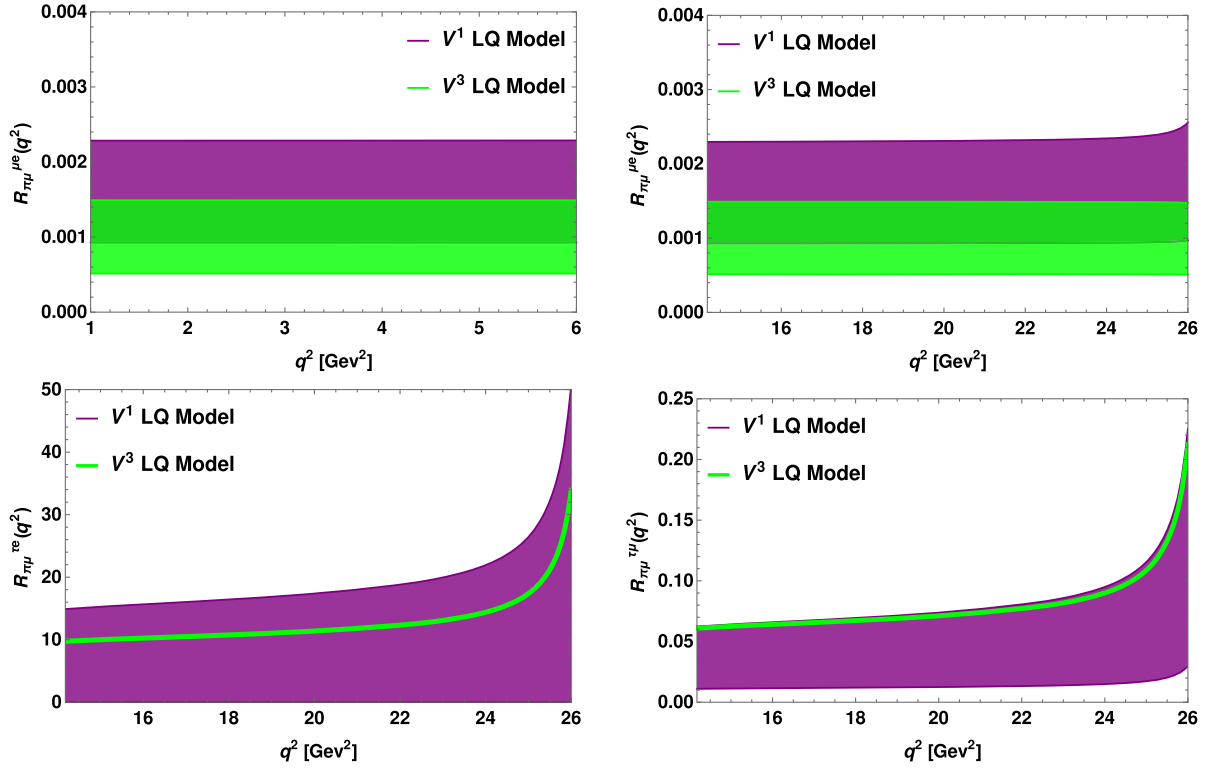


FIG. 15. The q^2 variations of $R_{\pi\mu}^{\mu e}$ (top right panel), $R_{\pi\mu}^{\tau e}$ (bottom left panel) and $R_{\pi\mu}^{\tau\mu}$ (bottom right panel) parameters in high q^2 region in the leptoquark model. Here $R_{\pi\mu}^{\mu e}$ (top left panel) shows the lepton nonuniversality for low $q^2 \in [1, 6]$ region.

$$a_\mu^{\text{SM}} = 116591785(61) \times 10^{-11}, \quad (102)$$

has the discrepancy

$$\Delta a_\mu = a_\mu^{\text{exp}} - a_\mu^{\text{SM}} = (295 \pm 88) \times 10^{-11}. \quad (103)$$

TABLE VI. The predicted values of forward-backward asymmetries and lepton nonuniversality parameters in $B \rightarrow \pi l_i^- l_j^+$ process in the $V^{1,3}$ vector leptoquark model. Also the predicted values of $R_\pi^{\mu\mu}$, $R_{\pi e}^{l_j l_j}$, $R_{\pi\mu}^{l_j l_j}$ parameters for muonic (electronic) processes in low $q^2 \in [1, 6]$ region.

Observables	Values in V^1 LQ model	Values in V^3 LQ model
$\langle A_{FB}^{\pi\mu e} \rangle$	$(0.432-4.42) \times 10^{-3}$	2.4×10^{-3}
$\langle A_{FB}^{\pi\tau e} \rangle$	0.2632	0.263
$\langle A_{FB}^{\pi\tau\mu} \rangle$	0.263-0.271	0.26
$\langle R_\pi^{\mu\mu} \rangle _{q^2 \in [1,6]}$	$1.084 \times 10^{-7}-1.95$	1.655×10^{-7}
$\langle R_\pi^{\mu\mu} \rangle$	$1.09 \times 10^{-7}-0.6$	1.66×10^{-7}
$\langle R_{\pi e}^{\mu e} \rangle _{q^2 \in [1,6]}$	$2.48 \times 10^{-10}-1.8 \times 10^{-3}$	2.46×10^{-10}
$\langle R_{\pi e}^{\mu e} \rangle$	$2.5 \times 10^{-10}-5.5 \times 10^{-4}$	2.47×10^{-10}
$\langle R_{\pi e}^{\tau e} \rangle$	$(0.0187-1.53) \times 10^{-4}$	1.86×10^{-6}
$\langle R_{\pi e}^{\tau\mu} \rangle$	$3.75 \times 10^{-9}-7.33 \times 10^{-3}$	3.6×10^{-9}
$\langle R_{\pi\mu}^{\mu e} \rangle _{q^2 \in [1,6]}$	$(1.8-2.29) \times 10^{-3}$	1.492×10^{-3}
$\langle R_{\pi\mu}^{\mu e} \rangle$	$(0.932-2.3) \times 10^{-3}$	1.49×10^{-3}
$\langle R_{\pi\mu}^{\tau e} \rangle$	$2.57 \times 10^{-4}-17.14$	11.23
$\langle R_{\pi\mu}^{\tau\mu} \rangle$	0.0123-0.073	0.07

The absolute magnitude of the discrepancy is small and can be accommodate by adding the new physics contributions. The vector LQ contribution to a_μ is given by

$$\begin{aligned} \Delta a_\mu = & -2N_c m_\mu \left[(g_L)_{b\mu} (g_R)_{b\mu}^* \left(-\frac{1}{3} (f_3(x_b) + f_4(x_b)) \right. \right. \\ & \left. \left. + \frac{2}{3} (\bar{f}_3(x_b) + \bar{f}_4(x_b)) \right) \right. \\ & \left. + (|(g_L)_{b\mu}|^2 + |(g_R)_{b\mu}|^2) \left(-\frac{1}{3} f_1(x_b) + \frac{2}{3} \bar{f}_1(x_b) \right) \right] \\ & - 2N_c m_\mu (|(g_L)_{b\mu}|^2 + |(g_R)_{b\mu}|^2) \\ & \times \left(-\frac{1}{6} f_1(x_b) + \frac{1}{3} \bar{f}_1(x_b) \right), \quad (104) \end{aligned}$$

where the loop functions are given in Sec. VC. Now using the constrained leptoquark couplings from $\tau^- \rightarrow \mu^- \gamma$ process with the scaling law as discussed in section VI, Δa_μ in the leptoquark model is found as

$$2.38 \times 10^{-9} \leq \Delta a_\mu \leq 2.95 \times 10^{-9}, \quad (105)$$

which is within its 1σ range.

VIII. CONCLUSION

In this work, we have studied the rare lepton flavor violating semileptonic B meson decays in the vector leptoquark model. These decays occur at loop level with a tiny neutrino mass in one of the loops, and are thus extremely rare in the SM but can occur at tree level in the vector leptoquark model. There are three vector leptoquarks which are relevant when studying the processes mediated via $b \rightarrow (s, d)$ transitions. Of these, we consider the $(3, 3, 2/3)$ and $(3, 1, 2/3)$ vector leptoquarks in our analysis and constrain the leptoquark couplings from $B_{s,d} \rightarrow l^+ l^-$, $K_L \rightarrow l^+ l^-$, and $\tau^- \rightarrow l^- \gamma$ processes, where l can be any charged leptons. Using such constrained parameters, we estimated the branching ratios and forward-backward asymmetries of $B \rightarrow K l_i^- l_j^+$ and $B \rightarrow \pi l_i^- l_j^+$ processes in the vector leptoquark model. We also

computed some parameters like $R_{K(\pi)e}^{l_i l_j}$, $R_{K(\pi)\mu}^{l_i l_j}$ and $R_+^{l_i l_j}$ (the ratios of various combination of rare decays) in order to inspect the presence of lepton nonuniversality. We also study the effect of vector leptoquark on the muon $g-2$ anomaly. We found that our predicted values are sizeable and within the reach of currently running or upcoming experimental limits, the observation of which in the LHCb experiment would provide a univocal signal of new physics.

ACKNOWLEDGMENTS

R.M. and S.S. would like to thank the Science and Engineering Research Board (SERB), Government of India, for financial support through Grant No. SB/S2/HEP-017/2013.

-
- [1] S. Descotes-Genon, J. Matias, M. Ramon, and J. Virto, *J. High Energy Phys.* **01** (2013) 048.
- [2] R. Aaij *et al.* (LHCb Collaboration), *Phys. Rev. Lett.* **111**, 191801 (2013).
- [3] R. Aaij *et al.* (LHCb Collaboration), *J. High Energy Phys.* **06** (2014) 133.
- [4] R. Aaij *et al.* (LHCb Collaboration), *Phys. Rev. Lett.* **113**, 151601 (2014).
- [5] C. Bobeth, G. Hiller, and G. Piranishvili, *J. High Energy Phys.* **12** (2007) 040.
- [6] R. Aaij *et al.* (LHCb Collaboration), *J. High Energy Phys.* **07** (2013) 084.
- [7] S. L. Glashow, D. Guadagnoli, and K. Lane, *Phys. Rev. Lett.* **114**, 091801 (2015).
- [8] V. Khachatryan *et al.* (CMS Collaboration), *Phys. Lett. B* **749**, 337 (2015).
- [9] Chao-Jung Lee and J. Tandean, *J. High Energy Phys.* **08** (2015) 123; W. Altmannshofer and I. Yavin, *Phys. Rev. D* **92**, 075022 (2015); A. Crivellin, G. D'Ambrosio, and J. Heeck, *Phys. Rev. Lett.* **114**, 151801 (2015); L. Calibbi, A. Crivellin, and T. Ota, *Phys. Rev. Lett.* **115**, 181801 (2015); R. Alonso, B. Grinstein, and J.M. Camalich, [arXiv:1505.05164](https://arxiv.org/abs/1505.05164); A. Crivellin, L. Hofer, J. Matias, U. Nierste, S. Pokorski, and S. Rosiek, *Phys. Rev. D* **92**, 054013 (2015) [[arXiv:1504.07928](https://arxiv.org/abs/1504.07928)].
- [10] S. Sahoo and R. Mohanta, *Phys. Rev. D* **93**, 114001 (2016).
- [11] S. Sahoo and R. Mohanta, *Phys. Rev. D* **91**, 094019 (2015).
- [12] D. Becirevic, N. Kosnik, O. Sumensari, and R. Zukanovich Funchal, [arXiv:1608.07583](https://arxiv.org/abs/1608.07583).
- [13] K. A. Olive *et al.* (Particle Data Group Collaboration), *Chin. Phys. C* **38**, 090001 (2014).
- [14] H. Georgi and S.L. Glashow, *Phys. Rev. Lett.* **32**, 438 (1974); J.C. Pati and A. Salam, *Phys. Rev. D* **10**, 275 (1974).
- [15] H. Georgi, *AIP Conf. Proc.* **23**, 575 (1975); H. Fritzsch and P. Minkowski, *Ann. Phys. (N.Y.)* **93**, 193 (1975); P. Langacker, *Phys. Rep.* **72**, 185 (1981).
- [16] D. B. Kaplan, *Nucl. Phys.* **B365**, 259 (1991).
- [17] B. Schrempp and F. Shrempp, *Phys. Lett. B* **153**, 101 (1985); B. Gripaios, *J. High Energy Phys.* **02** (2010) 045.
- [18] R. Mohanta, *Phys. Rev. D* **89**, 014020 (2014).
- [19] S. Davidson, D.C. Bailey, and B. A. Campbell, *Z. Phys. C* **61**, 613 (1994); I. Dorsner, S. Fajfer, J. F. Kamenik, and N. Kosnik, *Phys. Lett. B* **682**, 67 (2009); S. Fajfer and N. Kosnik, *Phys. Rev. D* **79**, 017502 (2009); R. Benbrik, M. Chabab, and G. Faisel, [arXiv:1009.3886](https://arxiv.org/abs/1009.3886); A. V. Povarov and A. D. Smirnov, [arXiv:1010.5707](https://arxiv.org/abs/1010.5707); J. P. Saha, B. Misra, and A. Kundu, *Phys. Rev. D* **81**, 095011 (2010); I. Dorsner, J. Drobnak, S. Fajfer, J. F. Kamenik, and N. Kosnik, *J. High Energy Phys.* **11** (2011) 002; F. S. Queiroz, K. Sinha, and A. Strumia, *Phys. Rev. D* **91**, 035006 (2015); B. Allanach, A. Alves, F. S. Queiroz, K. Sinha, and A. Strumia, *Phys. Rev. D* **92**, 055023 (2015); R. Alonso, B. Grinstein, and J.M. Camalich, *J. High Energy Phys.* **10** (2015) 184; Ivo de M. Varzielas and G. Hiller, *J. High Energy Phys.* **06** (2005) 072; M. Bauer and M. Neubert, *Phys. Rev. Lett.* **116**, 141802 (2016); S. Fajfer and N. Kosnik, *Phys. Lett. B* **755**, 270 (2016); I. Dorsner, S. Fajfer, A. Greljo, J. F. Kamenik, and N. Kosnik, *Phys. Rep.* **641**, 1 (2016); S.-w. Wang and Ya-dong Yang, *Adv. High Energy Phys.* **2016** (2016) 5796131; D. Aristizabal Sierra, M. Hirsch, and S. G. Kovalenko, *Phys. Rev. D* **77**, 055011 (2008); K. S. Babu and J. Julio, *Nucl. Phys.* **B841**, 130 (2010); S. Davidson and S. Descotes-Genon, *J. High Energy Phys.* **11** (2010) 073; S. Fajfer, J. F. Kamenik, I. Nisandzic, and J. Zupan, *Phys. Rev. Lett.* **109**, 161801 (2012) [[arXiv:1206.1872](https://arxiv.org/abs/1206.1872)]; K. Cheung and D. A. Camargo, [arXiv:1509.04263](https://arxiv.org/abs/1509.04263); S. Baek and K. Nishiwaki, *Phys. Rev. D* **93**, 015002 (2016) [[arXiv:1509.07410](https://arxiv.org/abs/1509.07410)]; J.M. Arnold, B. Fornal, and M.B. Wise,

- Phys. Rev. D **88**, 035009 (2013), [arXiv:1304.6119]; D. A. Faroughy, A. Greljo, and J. F. Kamenik, Phys. Lett. B **764**, 126 (2017); D. Becirevic, S. Fajfer, N. Kosnik, and O. Sumensari, Phys. Rev. D **94**, 115021 (2016); C.-Hung Chen, T. Nomura, and H. Okada, Phys. Rev. D **94**, 115005 (2016); G. Kumar, Phys. Rev. D **94**, 014022 (2016); R. Barbieri, G. Isidori, A. Pattori, and F. Senia, Eur. Phys. J. C **76**, 67 (2016).
- [20] S. Sahoo and R. Mohanta, Phys. Rev. D **93**, 034018; New J. Phys. **18**, 013032 (2016); **18**, 093051 (2016); arXiv:1612.02543.
- [21] M. Freytsis, Z. Ligeti, and J. T. Ruderman, Phys. Rev. D **92**, 054018 (2015); I. Dorsner, S. Fajfer, J. F. Kamenik, and N. Kosnik, Phys. Lett. B **682**, 67 (2009); Xin-Q. Li, Ya-D. Yang, and X. Zhang, arXiv:1605.09308; B. Dumont, K. Nishiwaki, and R. Watanabe, Phys. Rev. D **94**, 034001 (2016) [arXiv:1603.05248]; S. Sahoo, R. Mohanta, and A. K. Giri, arXiv:1609.04367; G. Hiller, D. Loose, and K. Schönwald, J. High Energy Phys. **12** (2016) 027; B. Bhattacharya, A. Datta, J. Guevin, D. London, and R. Watanabe, J. High Energy Phys. **01** (2017) 015.
- [22] W. Buchmuller, R. Ruckl, and D. Wyler, Phys. Lett. B **191**, 442 (1987); **448**, 320(E) (1997).
- [23] N. Kosnik, Phys. Rev. D **86**, 055004 (2012).
- [24] I. Dorsner, S. Fajfer, A. Greljo, J. F. Kamenik, N. Kosnik, and I. Nisandzic, J. High Energy Phys. **06** (2015) 108; K. Cheung, W.-Y. Keung, and P.-Y. Tseng, Phys. Rev. D **93**, 015010 (2016); S. Baek and K. Nishiwaki, Phys. Rev. D **93**, 015002 (2016).
- [25] A. J. Buras and M. Munz, Phys. Rev. D **52**, 186 (1995); M. Misiak, Nucl. Phys. **B393**, 23 (1993); **439**, 461(E) (1995).
- [26] R. Aaij *et al.* (LHCb Collaboration) J. High Energy Phys. **12** (2012) 125.
- [27] A. J. Buras, R. Fleischer, J. Girrbach, and R. Knegjens, J. High Energy Phys. **07** (2013) 77.
- [28] K. De Bruyn, R. Fleischer, R. Knegjens, P. Koppenburg, M. Merk, A. Pellegrino, and N. Tuning, Phys. Rev. Lett. **109**, 041801 (2012).
- [29] C. Bobeth, M. Gorbahn, T. Hermann, M. Misiak, E. Stamou, and M. Steinhauser, Phys. Rev. Lett. **112**, 101801 (2014).
- [30] LHCb, CMS Collaboration, V. Khachatryan *et al.*, Nature (London) **522**, 68 (2015).
- [31] T. Aaltonen *et al.* (CDF Collaboration), Phys. Rev. Lett. **102**, 201801 (2009).
- [32] LHCb Collaboration, LHCb-CONF-2016-011, <https://cds.cern.ch/record/2220757>.
- [33] G. Isidori and R. Unterdorfer, J. High Energy Phys. **01** (2004) 009.
- [34] G. Buchalla and A. J. Buras, Nucl. Phys. **B412**, 106 (1994).
- [35] M. Misiak and J. Urban, Phys. Lett. B **451**, 161 (1999); G. Buchalla and A. J. Buras, Nucl. Phys. **B548**, 309 (1999).
- [36] L. Lavoura, Eur. Phys. J. C **29**, 191 (2003).
- [37] J. A. Bailey *et al.* (Fermilab Lattice and MILC Collaborations), Phys. Rev. D **93**, 025026 (2016).
- [38] A. Khodjamirian, T. Mannel, N. Offen, and Y.-M. Wang, Phys. Rev. D **83**, 094031 (2011).
- [39] B. Gripaios, M. Nardecchia, and S. A. Renner, J. High Energy Phys. **05** (2015) 006; S. Davidson, G. Isidori, and S. Uhlig, Phys. Lett. B **663**, 73 (2008); M. Redi, J. High Energy Phys. **09** (2013) 060.
- [40] G. W. Bennett *et al.* (Muon g-2 Collaboration), Phys. Rev. Lett. **92**, 161802 (2004).
- [41] J. P. Miller, E. de Rafael, and B. L. Roberts, Rep. Prog. Phys. **70**, 795 (2007).